

Lipid remodeling in phytoplankton exposed to multi-environmental drivers in a mesocosm experiment

Sebastian I. Cantarero¹, Edgart Flores¹, Harry Allbrook¹, Paulina Aguayo^{2,3,4}, Cristian A. Vargas^{3,5}, John E. Tamanaha⁶, J. Bentley C. Scholz⁶, Lennart T. Bach⁷, Carolin R. Löscher^{8,9}, Ulf Riebesell¹⁰, Balaji Rajagopalan¹¹, Nadia Dildar¹, Julio Sepúlveda^{1,5}

¹Department of Geological Sciences and Institute of Arctic and Alpine Research (INSTAAR), University of Colorado Boulder, Boulder, CO 80309, USA

²Departamento de Oceanografía, Universidad de Concepción, Casilla 160-C, Concepción, Chile

³Department of Aquatic System, Faculty of Environmental Sciences & Environmental Sciences Center EULA Chile, Universidad de Concepción, Concepción 4070386, Chile

⁴Institute of Natural Resources, Faculty of Veterinary Medicine and Agronomy, Universidad de Las Américas, Sede Concepcion, Chacabuco 539, Concepcion 3349001, Chile

⁵Millennium Institute of Oceanography (IMO), Universidad de Concepción, Concepción 4070386, Chile

⁶Laboratory for Interdisciplinary Statistical Analysis, Department of Applied Mathematics, University of Colorado, Boulder, Boulder CO, 80309, USA

⁷Institute for Marine and Antarctic Studies, University of Tasmania, Hobart, TAS 7004, Australia

⁸Nordcee, Department of Biology, University of Southern Denmark, Odense, Denmark

⁹Danish Institute for Advanced Study, University of Southern Denmark, Odense, Denmark

¹⁰Marine Biogeochemistry, GEOMAR Helmholtz Centre for Ocean Research Kiel, Düsternbrooker Weg 20, D-24105, Kiel, Germany

¹¹Department of Civil, Environmental, and Architectural Engineering, University of Colorado-Boulder, Boulder, CO, USA

Correspondence to: Sebastian I. Cantarero (sebastian.cantarero@colorado.edu)

Abstract. Lipid remodeling, the modification of cell membrane chemistry via structural rearrangements within the lipid pool of an organism, is a common physiological response amongst all domains of life to alleviate environmental stress and maintain cellular homeostasis. Whereas culture experiments and environmental studies of phytoplankton have demonstrated the plasticity of lipids in response to specific abiotic stressors, few analyses have explored the impacts of multi-environmental stressors at the community-level scale. Here, we study changes in the pool of intact polar lipids (IPLs) of a phytoplanktonic community exposed to multi-environmental stressors during a ~2-month long mesocosm experiment deployed in the eastern tropical South Pacific off the coast of Callao, Perú. We investigate lipid remodeling of IPLs in response to changing nutrient stoichiometries, temperature, pH, and light availability in surface and subsurface water-masses with contrasting redox potentials, using multiple linear regressions, classification and regression trees, and random forest analyses. We observe proportional increases of certain glycolipids (namely mono- and di-galactosyldiacylglycerols; MGDG and DGDG, respectively) associated with higher temperatures and oxic conditions, consistent with previous observations of their utility to compensate for thermal stress, and their degradation under oxygen stress. N-bearing (i.e., betaine lipids and phosphatidylethanolamine; BL and PE) and non-N-bearing (i.e., MGDG, phosphatidylglycerol, and sulfoquinovosyldiacylglycerol; PG, SQDG) IPLs are anti-correlated, and have strong positive correlations with nitrogen repleted and depleted conditions, respectively, which suggests a substitution mechanism for N-bearing IPLs under nitrogen limitation. Reduced CO₂(aq) availability and increased pHs are associated with greater proportions of DGDG and sulfoquinovosyldiacylglycerol (SQDG) IPLs, possibly in response to the lower concentration of CO₂(aq) and the overall lower availability of inorganic carbon for fixation. A higher production of MGDG in surface waters corresponds well with their established photoprotective and antioxidant mechanisms in thylakoid membranes. The observed statistical relationships between IPL distributions, physicochemical parameters, and the composition of the phytoplankton community suggest

45 evidence of lipid remodeling in response to environmental stressors. These physiological responses may allow phytoplankton
46 to reallocate resources from structural or extrachloroplastic membrane lipids (i.e., phospholipids and betaine lipids) under
47 high-growth conditions, to thylakoid/plastid membrane lipids (i.e., glycolipids and certain phosphatidylglycerols) under
48 growth-limiting conditions. Further investigation of the exact mechanisms controlling the observed trends in lipid distributions
49 are necessary to better understand how membrane reorganization under multi-environmental stressors can affect the pools of
50 cellular C, N, P, and S, as well as their fluxes to higher trophic levels in marine environments subjected to increasing
51 environmental pressure. Our results suggest that future studies addressing the biogeochemical consequences of climate change
52 in the Eastern Tropical South Pacific Ocean must take into consideration the impacts of lipid remodeling in phytoplankton.

53 **1 Introduction**

54 The Eastern Tropical South Pacific (ETSP) is one of the most productive eastern boundary upwelling systems in the world
55 (Chavez and Messié, 2009) and harbors one of the largest oxygen deficient zones (ODZs) (Fuenzalida et al., 2009; Ulloa and
56 Pantoja, 2009; Thamdrup et al., 2012). Global warming has led to the expansion of ODZs over the recent decades and they are
57 expected to continue expanding due to the reduction in oxygen solubility with increasing temperature (Stramma et al., 2008;
58 Stramma et al., 2010; Gilly et al., 2013), as well as because of enhanced ocean stratification and reduced ventilation of the
59 ocean's interior (Keeling et al., 2010). The future behavior of the ETSP upwelling system in a warmer world remains uncertain;
60 increases in wind-induced upwelling intensity and duration (Gutiérrez et al., 2011; Bakun et al., 2010) may increase the supply
61 of nutrients to the surface in coastal regions, whereas enhanced thermal stratification may reduce nutrient supply in the open
62 ocean (Behrenfeld et al., 2006). Furthermore, upwelling regions are prone to highly variable pH (Capone and Hutchins, 2013),
63 and the global ocean will experience a decreasing average pH as more CO₂ accumulates in the atmosphere and is absorbed by
64 the ocean (Jiang et al., 2019). Accordingly, major shifts in marine planktonic community composition, turnover rates (Henson
65 et al., 2021), and adaptations (Irwin et al., 2015) are expected in future scenarios of ocean conditions, which are expected to
66 lead to cascading effects on ocean biogeochemistry and marine ecosystems (Hutchins and Fu, 2017).

67
68 Primary productivity in the ETSP is predominantly regulated by the wind-induced upwelling of nutrients, light availability,
69 and Fe limitation (Messié and Chavez, 2015). Thus, changes in the supply of inorganic N along the upwelling region of the
70 ETSP are likely to induce significant shifts in the phytoplankton community composition. Longer upwelling seasons along
71 nearshore environments could further stimulate productivity of fast-growing eukaryotic algae that currently dominate these
72 systems (e.g., diatoms; Messié et al., 2009). However, shorter upwelling seasons or weaker upwelling currents could favor
73 more survivalist or mixotrophic algae, in addition to N-fixing diazotrophs that thrive under widespread nitrogen limitation
74 (Dutkiewicz et al., 2012). The rate of primary productivity in the surface ocean not only affects the supply of sinking organic
75 matter and thus oxygen consumption via microbial respiration in the subsurface (Wyrski, 1962), but also results in a shift of
76 redox potentials that drive substantial losses of bioavailable N under reducing conditions at intermediate depths (Lam et al.,
77 2009; Wright et al., 2012). Additionally, expected changes in ocean warming and stratification (Huertas et al., 2011; Morán et
78 al., 2010; Yvon-Durocher, 2015), lowered dissolved oxygen concentration (Wu et al., 2012), and decreased pH (Dutkiewicz
79 et al., 2015, Bach et al., 2017), will disrupt phytoplanktonic assemblages differently based on their individual tolerances and

80 physiological plasticity. However, little is known of the physiological adaptations of phytoplankton on a community-level
81 scale in response to multi environmental stressors.

82

83 Phytoplankton have been shown to activate several lipid-based physiological mechanisms in response to environmental stimuli
84 (Li-Beisson et al., 2019; Sayanova et al., 2017; Kong et al., 2018). In fact, intact Polar Lipids (IPLs) are a class of membrane
85 lipids characterized by a polar head group typically attached to a glycerol backbone from which aliphatic chains are attached
86 via ester and/or ether bonds (Sturt et al., 2004; Lipp et al., 2008; Schubotz et al., 2009; Van Mooy and Fredricks, 2010).
87 Dominant planktonic lipid classes include phospholipids with a phosphate-bearing polar head group (e.g., phosphatidylcholine
88 PC; phosphatidylethanolamine PE; and Phosphatidylglycerol PG), glycolipids featuring a sugar moiety in the polar head (e.g.,
89 monoglycosyldiacylglycerol MGDG; diglycosyldiacylglycerol DGDG; sulfoquinovosyldiacylglycerol SQDG), and betaine
90 lipids with a quaternary amine positively charged and attached to lipid chains (e.g. diacylglyceryl hydroxymethyl-trimethyl-
91 β -alanine DGTA; diacylglyceryl trimethylhomoserine DGTS; and diacylglycerylcarboxy-N-hydroxymethyl-choline DGCC)
92 (Kato et al., 1996; Rütters et al., 2001; Zink et al., 2003; Suzumura, 2005; Van Mooy et al., 2006). The remodeling of IPLs,
93 the main constituents of cell and organellar membranes, provides numerous physiological adjustments to attenuate
94 environmental stressors impacting phytoplankton (Zienkiewicz et al., 2016). These include nutrient limitation (Van Mooy et
95 al., 2009; Meador et al., 2017; Abida et al., 2015; Wang et al., 2016), homeoviscous regulation in response to changing
96 temperature (Sato et al., 1980; Sinensky, 1974; Neidleman, 1987) and pH (Tatsuzawa and Takizawa 1996; Poerschmann et
97 al., 2004; Guckert and Cooksey, 1990; Jin et al., 2021), or photosynthetic function under varying light availability (Sato et al.,
98 2003; Gašparović et al., 2013; Khotimchenko and Yakovleva, 2005). While IPL distributions in environmental studies are
99 typically used as chemotaxonomic biomarkers that trace the presence and abundance of specific microbial groups (Sturt et al.,
100 2004; Schubotz et al., 2009; Van Mooy and Fredricks, 2010), their distributions have been used in conjunction with additional
101 microbial or geochemical measurements to assess how microbial metabolisms contribute to the chemical environment (Van
102 Mooy et al., 2009; Wakeham et al., 2012; Schubotz et al., 2018; Cantarero et al., 2020). Yet, few studies have explored how
103 multiple environmental drivers impact IPL remodeling at the community level and in time series, and the associated
104 adaptability of phytoplankton to environmental change.

105

106 Lab-based culture experiments have been a major step forward in understanding how lipid remodeling may impact a
107 biogeochemical system (as summarized above). However, a significant challenge remains in contextualizing these findings at
108 the community scale. Conversely, observational studies from direct measurements of natural systems are often logistically
109 limited in temporal scale, and consequently, do not fully capture the dynamics and heterogeneity of biogeochemical conditions.
110 Mesocosms are experimental apparatuses at the interface between controlled culture experiments and environmental
111 observations that allow for the examination of natural systems and entire ecosystems under semi-controlled conditions to
112 explore the impacts of a changing climate and ocean system (Riebesell et al., 2013). Here, we study changes in the composition,
113 diversity, and abundance of phytoplanktonic IPLs in response to changes in the biological, physical, and chemical composition

114 of a marine ecosystem subjected to semi-controlled conditions in a 2-month long mesocosm experiment off the coast of Perú.
115 We investigate the potential for IPL remodeling amongst phytoplankton in response to multiple environmental stressors
116 including nutrient availability, O₂ concentration, pH, temperature, and light availability to highlight adaptation strategies
117 available to phytoplankton in response to a changing ocean system.
118

119 **2 Methods**

120 **2.1 Mesocosm Deployment and Sampling**

121 On February 22, 2017, eight “Kiel Off-Shore Mesocosms for Ocean Simulations” (KOSMOS; Riebesell et al., 2013) were
122 deployed just north of Isla San Lorenzo, 6 km off the Peruvian coastline (12.0555° S, 77.2348° W; Fig. 1; Bach et al., 2020)
123 in waters 30 m deep. Each individual mesocosm consisted of a cylindrical polyurethane bag (2 m diameter, 18.7 m length,
124 54.4 ± 1.3 m³ volume) suspended in an 8 m tall flotation frame. Water exchange was permitted via nets (mesh size 3mm) for
125 three days before the water mass inside each mesocosm was enclosed and isolated from the surrounding Pacific water by
126 attaching sediment traps at the base (~19 m length total). The enclosing of the mesocosms marked the start (day 0) of the 50-
127 day experiment. As detailed in Bach et al. (2020), the experiment involved several manipulations including the addition of
128 ODZ water to simulate upwelling conditions, salt to maintain water stratification, and the introduction of organisms.
129

130 The collection of subsurface waters and their addition to the mesocosms is described with detail in Bach et al. (2020). Briefly,
131 on experiment days 5 and 10, two batches of local subsurface ODZ water were collected from stations with varying nutrient
132 stoichiometries (Table 1; Fig. 1) using deepwater collectors first reported by Taucher et al., (2017). The water mass collected
133 from 30 m deep at station 1 (12.028323° S, 77.223603° W) was characterized by a very low N:P ratio (Table 1), whereas the
134 water collected from 70 m deep at station 3 (12.044333° S, 77.377583° W) was characterized by a higher but still low N:P
135 ratio (Table 1). On experiment day 8, 9 m³ of water was removed from each mesocosm at a depth between 11 and 12 m and
136 then on day 11, 10 m³ of ODZ water was injected into each mesocosm at depths between 14 and 17 m. On experiment day 12,
137 the entire procedure was repeated but this time with 10 m³ removed between 8 and 9 m, and 12 m³ added evenly between 1
138 and 9 m. To maintain stratification and preserve the low O₂ subsurface layer, a NaCl brine solution was injected evenly into
139 the subsurface of all mesocosms on experiment day 13 (0.067 m³, 10 to 17 m depth) and experiment day 33 (0.046 m³, 12.5 to
140 17 m depth). On day 14, Peruvian Scallop larvae (*Argopecten purpuratus*) were added (~10,000 individuals m⁻³), and on day
141 31 Fine Flounder eggs (*Paralichthys adspersus*) were added (~90 individuals m⁻³). However, few scallop larvae and no fish
142 larvae were found in the mesocosms after the release indicating that their influence on the plankton community was likely
143 small (Bach et al., 2020).
144

145 We sampled two integrated water depths of the mesocosms for suspended organic matter and biological and chemical
146 characterization using 5 L integrating water samplers (IWSs; Hydro-Bios, Kiel) equipped with pressure sensors to collect water
147 evenly within a desired depth range. The samples were collected across two integrated intervals of the water column
148 representing surface and subsurface layers, sampling depths were slightly modified over the course of the experiment to
149 accommodate for changes in water stratification and the position of the chemocline (refer to Bach et al., 2020 for further
150 details). The depths applied for surface and subsurface waters were 0–5 and 5–17 m on days 1 and 2, 0–10 and 10–17 m from
151 day 3 to 28, and 0–12.5 and 12.5–17 m from day 29 to 50.

152
153 Samples of suspended organic matter for IPL analysis were collected from all 8 mesocosms at both the surface and subsurface
154 sampling depths on non-consecutive days throughout the experiment. See details of changes in water depths above. Due to the
155 labor- and time-intensive nature of IPL analysis, we focused on 4 mesocosms (two from each treatment) at both depths and
156 from 9 different days spanning the 50-day experiment. We filtered 5 L of mesocosm water through pre-combusted, 142 mm
157 Advantec glass fiber filters (GF75142MM) of 0.3 μm pore size. All samples were wrapped in combusted aluminum foil and
158 shipped frozen to the Organic Geochemistry Laboratory at the University of Colorado, Boulder for IPL extraction and analysis.

159 **2.2 Water Column Physicochemistry**

160 Depth profiles of salinity, temperature, O_2 concentration, photosynthetically active radiation (PAR), and chlorophyll a (chl-a)
161 fluorescence were measured through vertical casts using the CTD60M sensor system (Sea & Sun Technology). O_2
162 concentrations were cross-verified with the Winkler O_2 titration method performed via a micro-Winkler titration method
163 described by Aristegui and Harrison (2002). Seawater pH_T (pH on total scale), was determined spectrophotometrically using
164 m-cresol purple (mCP) indicator dye as described in Carter, et al. (2013); see Chen et al. (2022) for details. See Bach et al.
165 (2020) for additional detailed information of sampling methods for water column physicochemistry.

166
167 Samples for inorganic nutrients were filtered immediately upon arrival at the laboratories at the Instituto del Mar del Perú
168 (IMARPE) using 0.45 μm Sterivex filter (Merck). The subsequent analysis was carried out using a continuous flow analyzer
169 (QuAatro AutoAnalyzer, SEAL Analytical) connected to a fluorescence detector (FP-2020, JASCO). The method for
170 analyzing PO_4^{3-} followed the procedure outlined by Murphy and Riley (1962), while $\text{Si}(\text{OH})_4$ was analyzed according to Mullin
171 and Riley (1955). NO_3^- and NO_2^- were quantified through the formation of a pink azo dye as established by Morris and Riley
172 (1963) and additional corrections to all colorimetric methods was achieved with the refractive index method developed by
173 Coverly et al. (2012). Ammonium concentrations were determined fluorometrically following the method of K erouel and
174 Aminot (1997). Further methodological specifics and the respective limits of detection for each analysis can be found in Bach
175 et al. (2020).

176 **2.3 CHEMTAX Analysis**

177 Pigment samples were flash-frozen in liquid nitrogen directly after filtration and kept frozen on dry ice during transport to
178 Germany for extraction as described by Paul et al. (2015). Concentrations of extracted pigments were measured by reverse-
179 phase high-performance liquid chromatography (HPLC; Barlow et al., 1997) calibrated with commercially available standards.
180 The relative contribution of distinct phytoplankton taxa was calculated with CHEMTAX, a program for calculating the
181 taxonomic composition of phytoplankton populations (Mackey et al., 1996). Input pigment ratios specific to the Peruvian
182 upwelling system, determined by DiTullio et al. (2005) and further described by Meyer et al. (2017), were incorporated in
183 these calculations (see Bach et al., 2020).

184 **2.4 Flow Cytometry**

185 Samples (650 μL) from each mesocosm were analyzed using an Accuri C6 (BD Biosciences) flow cytometer. The signal
186 strength of the forward light scatter was used to distinguish phytoplankton groups, in addition to the light emission from red
187 fluorescence of chl-a, and the light emission from orange fluorescence of phycoerythrin. Size ranges were constrained via
188 gravity filtration using sequential polycarbonate filters ranging from 0.2 to 8 μm and the strength of the forward light scatter
189 signal. Additional details of this method can be found in Bach et al., 2017. In this study, we only report *Synechococcus* (0.8-3
190 μm) counts (cells mL^{-1}) because it is the only phytoplankton group that was consistently selected to exhibit statistically
191 significant trends with IPLs likely due to the non-size fractionated nature of IPL sampling.

192 **2.5 Lipid Extraction and Analysis**

193 Intact polar lipids were extracted from glass fiber filters via a modified version (Wörmer et al., 2015) of the original Bligh and
194 Dyer Extraction method (Bligh and Dyer, 1959). Samples were extracted by ultrasonication a total of five times, with three
195 different extraction mixtures. Two extractions were performed using Dichloromethane:Methanol:Phosphate buffer
196 (aq) [1:2:0.8, v:v:v], adjusted to a pH of ~ 7.4 , followed by another two extractions using
197 Dichloromethane:Methanol:Trichloroacetic acid buffer(aq) [1:2:0.8, v:v:v], adjusted to a pH of ~ 2.0 . A final extraction was
198 performed with Dichloromethane:Methanol [1:5, v:v]. After each addition, samples were vortexed for 30 s, sonicated for 10
199 min, and then centrifuged for 10 min at 3000 rpm while kept at 10 $^{\circ}\text{C}$. The supernatant of each extraction mixture was then
200 transferred to a separatory funnel where the organic fractions were washed and combined before solvent removal under a
201 gentle N_2 stream. Before analysis, the TLEs were resuspended in dichloromethane:methanol (9:1 v:v) and filtered through a
202 0.45 μm polytetrafluoroethylene (PTFE) syringe filter.

203
204 Chromatographic separation and identification of IPLs was achieved using a Thermo Scientific UltiMate 3000 high-
205 performance liquid chromatography (HPLC) interphase to a Q Exactive Focus Orbitrap-Quadrupole high resolution mass
206 spectrometer (HPLC-HRMS) via heated electrospray ionization (HESI) in positive mode, as described in detail in applications

207 by Cantarero et al. (2020) and Flores et al. (2022). Briefly, a flowrate of 0.4 ml/min was applied to an Aquity BEH Amide
208 column (150 mm, 2.1 mm, 1.7 μm) using a gradient program first described by Wörmer et al (2013). All filtered TLEs were
209 suspended in Dichloromethane:Methanol (9:1, v/v) prior to injection (10 μL) on column. The following HESI conditions were
210 applied; auxiliary gas temperature: 425 $^{\circ}\text{C}$, capillary temperature 265 $^{\circ}\text{C}$, spray voltage 3.5 kV, sheath gas flow rate: 35
211 arbitrary units (AU), auxiliary gas flow 13 AU, S-Lens RF level 55 AU. Samples were analyzed in full scan mode to obtain
212 an untargeted screening (or lipidomic profile) of each sample, in addition to targeted MS/MS mode for compound identification
213 via diagnostic fragmentation patterns (e.g., Sturt et al., 2004; Schubotz et al., 2009; Wakeham et al., 2012). IPLs were identified
214 by their exact masses, polar head groups, the total number of carbon atoms and unsaturations in the core structure, and their
215 retention times. While other studies have analyzed IPLs under both positive and negative ionization modes to determine the
216 composition of individual fatty acid chains in the core lipid structures, we took advantage of the high resolution of the Orbitrap
217 mass spectrometer to focus on the diversity of head group combinations with total carbon atoms and unsaturation only
218 (Cantarero et al., 2020).

219
220 Quantification of IPLs was achieved using a combination of an internal standard added (2 μg) to samples during extraction
221 (C16 PAF, Avanti Lipids), in addition to an external calibration curve consisting of 17 standards representing different IPL
222 classes (see Cantarero et al., 2020 for full details of all internal/external and deuterated standards). The intensity of each
223 individual IPL identified in the HPLC-HESI-HRMS analysis was calibrated to a linear regression between peak areas and
224 known concentrations of the same lipid class (or the most similar molecular structure) across a 5-point dilution series (0.0001–
225 10 ng/ μl). The detection limit, based on individual calibration curves, was determined to be 0.01 ng on column except for
226 DGTS (0.001 ng) and DGDG, MGDG, and SQDG classes (0.1 ng). Samples were analyzed across 3 separate analytical periods
227 with weekly calibration curves to account for variation in the ionization efficiency of compounds over time. Overall, HPLC-
228 ESI-HRMS is considered a semi-quantitative method due to changes in ionization efficiency of different IPL standards and
229 environmental analytes. These changes are largely caused by differences in polar head group compared to the acyl chain length
230 and degree of unsaturation (Yang and Han, 2011). Nonetheless, we investigate both relative (%) and absolute IPL abundances
231 to compensate for the current analytical limitations in IPL quantification.

232
233 While we report IPL structural variations associated with different head groups and modifications in the core structure (i.e.,
234 unsaturation degree and carbon length of diacyl chains), we particularly focus on the former. Additionally, several IPLs thought
235 to be absent in eukaryotic phytoplankton or far more abundant in bacteria and archaea ($n = 34$ in total) have been removed to
236 facilitate the analysis of trends that are predominantly phytoplanktonic in origin. These compounds include PME/PDME
237 (Phosphatidyl(di)methylethanolamine) and intact GDGTs (glycerol dialkyl glycerol tetraethers) classes. In addition, while we
238 lack detailed structural information of core individual fatty acids, their combined carbon atoms can be used to deduce short
239 (i.e. < 14 carbon atoms per chain) or odd numbered fatty acid chains typically found in bacteria (Volkman et al., 1989; Volkman
240 et al., 1998; Russell and Nichols, 1999; Jónasdóttir, 2019). Thus, compounds conventionally regarded as bacterial (34 in total)

241 were also removed to minimize their impact on the analysis of predominantly phytoplanktonic IPLs (165 in total). We
242 recognize that while this selection approach reduces the influence of non-eukaryotic lipids, we still cannot rule out an
243 undetermined contribution from heterotrophic bacteria to the IPL pool in this experiment. A summary of these IPL classes and
244 their acronyms is provided in Table 2.

245

246 **2.6 Multiple Linear Regression**

247 We performed multiple linear regression between 8 relevant environmental factors and 165 unique IPLs. With so many IPL-
248 environmental factor pairs to analyze, we used multiple linear regression (MLR) for quick and easily digestible outputs. In
249 each MLR model, the relative abundance of individual IPL molecules was employed as a response variable, with environmental
250 factors serving as predictor variables. Additionally, phytoplankton abundances were included to account for their linear effects
251 on IPL distributions. The rationale behind this inclusion lies in the understanding that variations in phytoplankton abundance
252 may exert a proportional and predictable impact on the abundance patterns of specific IPLs.

253

254 We prioritized linear relationships with IPL relative abundances (% abundances) to emphasize changes in the proportions of
255 phytoplankton lipids, rather than their absolute concentration and contribution to biomass. This approach enables us to
256 distinguish compositional changes in the lipid pool from variability in total biomass production. Additionally, MLRs were
257 constrained to focus on the most abundant IPLs in this system, defined as those constituting more than 2.5% to the total IPL
258 pool. This restriction was implemented to reduce noise associated with low-abundance IPLs and enhance the robustness of
259 analysis.

260

261 We chose to investigate linear relationships within individual depths (surface and subsurface) to focus on temporal changes
262 within distinct environments, rather than comparing these two environments directly (see CART and Random Forest methods,
263 below). IPLs and environmental factors were permuted to tabulate the regression coefficient for each IPL-environmental factor
264 pair. Model coefficients were directly comparable due to centering and scaling of environmental and phytoplankton variables
265 (see eq. 1) to linearize the relationship and better align with the model assumptions:

266

$$267 \quad Y = \beta_0 + \beta_1 X_1 + \beta_2 X_2 + \dots + \beta_n X_n + \varepsilon \quad \text{eq. (1)}$$

268 where, Y is the dependent variable (or response), X_1, X_2, \dots, X_n are the predictor variable (or independent variables), β_0 is the
269 intercept (constant term), $\beta_1, \beta_2, \dots, \beta_n$ are the coefficients representing the magnitude and direction of the relationship between
270 the predictor variable and the dependent variable, and ε is the error term capturing the variability not explained by the model.

271 Correlations in the MLR analysis were also controlled for false discovery rate following the procedure of Benjamini and
272 Hochberg, (1995) to calculate adjusted p-values and by applying an alpha cutoff of 0.1.

273

274 **2.7 Classification and Regression Tree (CART) and Random Forest**

275 Classification and Regression Trees (CART; Breiman et al., 1984) are predictive machine learning algorithms that partition
276 and fit data along a predictor axis into homogenous subsets of the dependent variable. Regression trees are used for dependent
277 variables with continuous values, while classification trees for categorical values. Here, we apply regression trees to diagnose
278 the environmental and biological variables that affect IPL concentrations by polar head group class. We limited the size of the
279 tree splits via a “pruning” process, where less significant variable splits are removed as determined by a deviance criterion
280 resulting in the best-fit tree with the least mean squared error. Additionally, predictor variables were selected in conjunction
281 with random forest analyses, which ranks the variable contribution to the model performance.

282

283 Random forests are derived from bootstrapping of observational data, and the generation of many decision trees based on each
284 bootstrap sample. We employed a total of 72 samples for the random forest analysis which was run separately for each major
285 IPL class (n = 7) to identify the most important environmental predictors (n = 12) for each individual class of lipid. The random
286 forest method utilizes bootstrap aggregation to generate and average numerous permutations of an out-of-bag score in
287 predictive performance. This approach offers an effective methodology for analyzing high-dimensional data with limited
288 sample sizes (Biau and Scornet, 2016). This method has been widely adopted across various disciplines within the water
289 sciences (Tyrallis, 2019), ecological and species distribution modeling (Luan et al., 2020), as well as in bioinformatics and
290 high-throughput genomics (Chen and Ishwaran, 2012; Boulesteix et al., 2012). For a covariate vector, the predicted estimate
291 of IPL class concentrations is an average of the many randomly configured decision trees with the same distribution. A
292 randomly generated subset of decision trees is used to split each node, enabling reduced variance and correlation amongst
293 individual trees, and ideally improving the accuracy of model predictions (Breiman, 2001). The random forest algorithm also
294 allows for the ranking of predictor variables based on the prediction performance and is reported here as the predictor’s
295 contribution in reducing the root mean square error (RMSE) in the model. For additional details on the random forest algorithm,
296 please see Hastie et al. (2009). All CHEMTAX, flow cytometry, and physicochemical variables were included in the CART
297 and random forest analyses as predictors. Regression tree (CART) splitting criteria are determined by evaluating the sum of
298 squared deviations in all possible splits and selecting those that result in the greatest reduction of residual error. To prevent
299 overfitting in the CART analysis, a pruning procedure is run to remove nodes that contribute little to the model accuracy based
300 on a cost complexity measure. This procedure allows us to simplify the CART results and thus focus our interpretations on the
301 most significant predictors of IPL headgroups only. In the Random Forest model, following the averaged cross validated
302 accuracy estimates, we implemented a cutoff of 5% reduction in RMSE to eliminate variables that do not significantly reduce

303 the error of the model prediction. This cutoff allows us to focus our interpretation of only variables that contribute significantly
304 to the out of bag predictor performance (For further details, refer to Supplementary Material, Note S1).
305 CART and random forest-based predictions serve as ideal methods to explore environmental drivers of IPL distributions- not
306 only because of their predictive performance- but also because of their non-parametric nature, their diagnosis of variable
307 importance, and their ability to handle non-linear interactions and small sample sizes (Tyrallis et al., 2019). We do not employ
308 these methods to predict the concentration of IPL classes, but rather to identify the primary environmental and biological
309 drivers of change in IPL class concentrations, and potential interactions between environmental conditions and IPL remodeling
310 amongst phytoplankton. Therefore, we focus our interpretations of both the CART and Random Forest analyses on only the
311 most significant predictors and their relative order of importance in the model predictions.

312 **3 Results**

313 **3.1 Oxygen and pH_T**

314 Oxygen concentration in surface waters ranged between ~125 and 140 $\mu\text{mol/L}$ before the ODZ water addition in all 4
315 mesocosms (Fig. 2A). The concentration dropped slightly (~15 $\mu\text{mol/L}$) following the water addition and steadily increased
316 to a maximum between ~185-220 $\mu\text{mol/L}$ by day 28. Day 30 marked a significant drop in oxygen concentration by 30-60
317 $\mu\text{mol/L}$ in all mesocosms with conditions stabilizing between 140 and 155 $\mu\text{mol/L}$ by day 50. The temporal variability in pH_T
318 in surface waters showed a largely mirrored trend to that of oxygen content. Before ODZ water addition pH_T was 7.9-8.0,
319 which dropped by ~0.2 immediately following the water addition. After a few days of relatively stable pH_T at ~7.8 in all four
320 mesocosms, the pH_T increased significantly between days 18 and 28 reaching ~8.1-8.2. From days 30-40 the pH_T gradually
321 decreased by approximately 0.2 in all mesocosms until increasing again (most notably in mesocosms 7 and 5) between days
322 42-50 to maxima ranging from 8.1-8.3.

323

324 The subsurface waters were more oxygen-depleted compared to the surface and showed an earlier onset of increasing oxygen
325 concentration, beginning immediately after the ODZ water addition. All four mesocosms reached maximum O₂ levels (60-75
326 $\mu\text{mol/L}$) by day 13 and began decreasing markedly by day 16. The lowest concentrations (~15 $\mu\text{mol/L}$ O₂) were reached
327 between days 30 and 34. Oxygen concentrations recovered slightly in the last 10-16 days of the experiment and were all within
328 30 (\pm 10) $\mu\text{mol/L}$ of O₂. The subsurface waters, again, showed similar temporal patterns in pH_T as with O₂, except for
329 mesocosm 7. The pH_T was variable (~7.60 \pm 0.05) in the early portion of the experiment (days 10-16) but did not show a
330 dramatic response to the OMZ water addition as was the case in the surface samples. The pH_T did gradually decrease from
331 days 18-30, with pH_T minima in all four mesocosms reached on day 30 (~7.45-7.50). Day 30 also marked the beginning of a
332 significant increase in the pH_T (~0.15-0.20) across all mesocosms with the pH_T steadily increasing to ~7.65-7.70 by day 50.
333 Additional details on the carbonate chemistry of the mesocosms can be found in Chen et al. (2022).

334

335 3.2 Nutrient Concentrations

336 In mesocosm surface waters, the nutrients NH_4^+ , NO_3^- , NO_2^- , PO_4^{3-} , and $\text{Si}(\text{OH})_4$ all showed consistent trends over time, with
337 the highest concentrations occurring either just before (day 10) or immediately after (day 12) the ODZ water addition (Fig.
338 2B). Nitrogen species ranged between 1 and 3 $\mu\text{mol/L}$ during this early part of the experiment, while $\text{Si}(\text{OH})_4$ ranged between
339 4 and 7 $\mu\text{mol/L}$, and PO_4^{3-} remained at $\sim 2 \mu\text{mol/L}$. The concentration of all nitrogen species dropped quickly to near minimum
340 values by day 15, and typically remained $<0.5 \mu\text{mol/L}$ for the remainder of the experiment. PO_4^{3-} remained replete (>1.5
341 $\mu\text{mol/L}$ for the entirety of the experiment). $\text{Si}(\text{OH})_4$ dropped to $\sim 3\text{-}4 \mu\text{mol/L}$ by day 15 and gradually increased in all 4
342 mesocosms by 1-2 $\mu\text{mol/L}$ until days 36-38, where concentrations gradually dropped to near minimum values of 3-4 $\mu\text{mol/L}$.
343 There were periodic enrichments in NH_4^+ , most notably between days 40-50, as discussed in Bach et al., 2020.

344
345 The mesocosm subsurface water nutrients showed similar temporal patterns as the surface but were generally more enriched
346 in all nutrient species. All nitrogen species decreased in the few days following the ODZ water addition, but at a more gradual
347 pace than in the surface. Before and immediately after the water addition, NO_3^- was enriched at 4-6 $\mu\text{mol/L}$ and NH_4^+ between
348 2.5-4 $\mu\text{mol/L}$. NO_2^- concentrations were $\sim 0.5\text{-}1 \mu\text{mol/L}$ in mesocosms 6 and 7 during this period but remained low (<0.3
349 $\mu\text{mol/L}$) in mesocosms 5 and 8. Broadly speaking, the nitrogen species all reached minimal values ($<0.1 \mu\text{mol/L}$) by days 18-
350 20, except for in mesocosms 6 and 8, where NO_3^- persisted at significant concentrations (0.2-2.3 $\mu\text{mol/L}$) until days 22 and
351 24, respectively. The remainder of the experiment was marked by typically depleted concentrations of all nitrogen species
352 ($<0.1 \mu\text{mol/L}$) with occasional spikes in NH_4^+ reaching up to 1 $\mu\text{mol/L}$, particularly towards the end of the experiment.
353 Subsurface PO_4^{3-} concentrations were similar to the surface, remaining around $\sim 2.0 \mu\text{mol/L}$ for most of the experiment which
354 gradually decreased to concentrations of $\sim 1.5 \mu\text{mol/L}$ by the end of the experiment. $\text{Si}(\text{OH})_4$ similarly decreased from
355 maximum concentrations of 4.0-4.5 $\mu\text{mol/L}$ shortly after the ODZ water addition, and gradually decreased by $\sim 1 \mu\text{mol/L}$ over
356 the course of the experiment.

357 3.3 Total Chlorophyll a

358 Chl-a concentrations were highly variable throughout the experiment, particularly in subsurface waters (Fig. 2C).
359 Concentrations were generally more elevated at the surface compared to the subsurface, with values ranging $\sim 2.56\text{-}2.96 \mu\text{g/L}$
360 on day 10. In all mesocosms, the chl-a concentration increased to $\sim 7.94\text{-}14.01 \mu\text{g/L}$ after the ODZ water addition and through
361 day 20. Day 22 showed a significant drop in chl-a concentrations to between 1.35 and 2.89 $\mu\text{g/L}$ in mesocosms 7, 5, and 8.
362 Chl-a concentrations at the surface remained rather constant until days 36-40, where concentrations rapidly increased until
363 maximum concentrations on days 48-50 (14.0-47.3 $\mu\text{g/L}$). In subsurface waters, chl-a concentrations were notably lower than
364 in the surface and ranged between 0.58-0.84 $\mu\text{g/L}$ on day 10. After the ODZ water addition, chl-a concentrations increased
365 slightly until day 14, but did not show consistent distributions amongst the 4 mesocosms afterwards; decreases were observed
366 in mesocosms 6, 5, and 8, but an increase in mesocosm 7. Chl-a concentrations increased rapidly on day 22 in all 4 mesocosms

367 ranging between 4.03 and 8.44 $\mu\text{g/L}$. While remaining highly variable, the concentrations generally increased after day 24
368 with a notably abrupt increase between days 40-44 to near maximum values ranging between 2.58-11.3 $\mu\text{g/L}$.

369 **3.4 Phytoplankton Community Composition**

370 The CHEMTAX based phytoplankton community compositions demonstrated more variability in phytoplankton assemblages
371 in the subsurface samples than in the surface (Fig. 2C). Before the ODZ water addition on day 10, surface waters in all 4
372 mesocosms showed similar phytoplankton distributions with high relative abundances of Bacillariophyceae, referred to from
373 here on as diatoms (20-45%), Chlorophyceae (15-50%), and Dinophyceae, referred to as dinoflagellates (25-45%). These
374 distributions remained rather similar immediately after the water addition (day 12), but dinoflagellate contributions increased
375 in the following days and ranged from ~20% of the total chl-a pool to up to 75% by day 20. Of note, Cryptophyceae made
376 minor contributions to the chl-a pool aside from days 15-18 in mesocosm 6 where they contributed up to 25%. Dinoflagellates
377 largely dominated the chl-a pool for the remainder of the experiment with moderate blooms of diatoms between days 34-44 in
378 mesocosms 7 and 8.

379
380 Subsurface waters exhibited greater variability in the phytoplankton assemblages and a greater contribution of Chlorophyceae,
381 Cryptophyceae, *Synechococcus*, and diatoms to the chl-a pool than in the surface. Pre-addition waters (day 10) were dominated
382 by diatoms making up >75% of the chl-a pool. In the first few days after the ODZ water addition (days 12-15), the relative
383 abundance of Chlorophyceae increased to 25-45% in mesocosms 6, 5 and 8, whereas Cryptophyceae contributed between 5-
384 15% of the total chl-a. During this period, diatoms continued to dominate mesocosm 7 but decreased gradually from 65 to 15%
385 of the phytoplankton community. Notably, in mesocosm 6, Cryptophyceae contributed a moderate amount to the chl-a pool
386 beginning on day 15 (25%) and gradually increased to 40% by day 20. Mesocosms 7, 5, and 8 increased in Cryptophyceae as
387 well, but were limited to ~10-25%. Similar to surface waters, dinoflagellates dominated the chl-a pool by day 20 and
388 contributed 50-80% of the chl-a pool; however, there was considerably greater variability in dinoflagellate abundance after
389 day 20 in subsurface waters. Chlorophyceae remained a significant contributor for the rest of the experiment typically ranging
390 between 10 and 25% of the phytoplankton relative abundance. In mesocosms 7, 5, and 8 diatoms became the dominant
391 contributor, totaling ~50% of the phytoplankton between days 32 and 44. By the final days of the experiment (days 48-50),
392 dinoflagellates again made up most of the phytoplankton community (60-75%). Pelagophyceae, Prymnesiophyceae, and
393 Cyanophyceae (referred to here as *Synechococcus*), remained minor contributors throughout the entire experiment but showed
394 maximum contributions of <10% in days 10-16. Mesocosm 6 showed a minor contribution (<10%) of *Synechococcus* from
395 days 42-50, and from days 34-42 in mesocosm 7.

396 **3.5 IPL Class Distributions**

397 The IPL distributions throughout the study can be summarized by the relative abundances of different classes determined by
398 their polar head groups. IPL distributions were broadly consistent between mesocosms and treatments during the experiment

399 but showed significant differences between surface and subsurface waters (Fig. 2D). Glycolipids such as SQDG, DGDG, and
400 MGDG typically made up ~50-75% of the total IPL pool in the surface, whereas phospholipids such as PC and PG were
401 dominant in the subsurface (~50-75%). The changes in IPL distribution from the surface samples over the course of the
402 experiment were most apparent between days 10 to 12, 20 to 24, and 24 to 38. Day 10 of the experiment marks the sampling
403 period immediately preceding the ODZ water addition and was the only day with a significant fraction of BLs (betaine lipids)
404 in the total lipid pool (ranging from 25-30% in the surface samples). Mesocosms 6 and 8 showed a similar distribution between
405 days 10 and 12 of the experiment with large contributions of SQDGs (~50%), BLs (~25-30%), and MGDGs (~20%), while
406 mesocosms 7 and 5 showed considerably more PCs (~25-40%) at the expense of SQDGs (<10%). In the 2 weeks following
407 the deep-water addition (days 12 to 24), we saw increasing (albeit variable) relative abundances of PGs (from 5 to 50%) and
408 DGDGs (from 5 to 25%) in surface waters. MGDGs made up a considerably larger fraction during this time in mesocosm 6
409 (up to 50%), but were more moderate in mesocosms 7, 5, and 8 (typically ~25%), yet decreased in all mesocosms to <5% by
410 day 24. The final sample days (38 and 50) showed a resurgence of glycolipid contributions, namely in SQDGs (25-55%) and
411 MGDGs (5-25%), with moderate contributions of PGs (5-20%) and DGDGs (5-20%).

412

413 In the subsurface samples before the ODZ water addition, mesocosms 6, 7, and 8 showed moderate contributions of MGDGs
414 (15-25%) which was lower in mesocosm 5 (<5%). There were higher contributions of SQDGs in mesocosms 6 and 8 (50%
415 and 35%, respectively) than in 7 and 5 (20-25%). Instead, mesocosms 7 and 5 showed a greater contribution of PCs (45-55%).
416 All 4 mesocosms demonstrated some component of PGs ranging from 5-20% of the total IPL pool. The 2 weeks following the
417 ODZ water addition showed highly variable fluctuations between PCs and PGs as the dominant IPL classes, with the
418 contributions of glycolipids (25-40%) and betaine lipids (<5%) remaining consistent. Of note, day 24 marked a consistently
419 low contribution of PCs, which persisted until the end of the experiment. The final sample days (38 and 50) showed similar
420 contributions between MGDGs, SQDGs, and PGs that together dominated the total lipid pool.

421 **3.6 Multiple Linear Regressions**

422 We found statistically significant ($p < 0.05$) linear relationships between the relative abundance of individual IPLs and
423 environmental factors (Figure 3). In surface waters, pH_T showed several significant responses towards DGDGs, MGDGs, PGs,
424 PEs and SQDGs. Classes DGDG, MGDG, PE and PG showed negative linear relationships with pH_T . SQDGs (specifically
425 SQDG-32:0), however, showed a strong positive linear response to pH_T . In the subsurface, pH_T only imparted significant linear
426 effects towards SQDGs with a strong negative linear correlation.

427

428 The temperature of surface waters showed predominantly positive regression coefficients with several PG, MGDG, and DGDG
429 molecules, with inconsistent correlations found in SQDGs. Whereas some PEs showed significant linear relationships with
430 temperature, their regression coefficients were near 0. Similarly, in the subsurface only 1 IPL structures (SQDG 34:3) showed
431 a significant positive linear response but with a regression coefficient near 0.

432

433 Oxygen concentrations showed few linear correlations at the surface and were limited to two BLs (negative) and 1 PG
434 (positive). In the subsurface, the strongest linear correlations were found between oxygen and PGs and SQDGs (negative).

435

436 Nutrient concentrations showed many significant linear responses with regression coefficients of higher magnitude (up to ± 8)
437 and adjusted R^2 values of up to 0.5. The concentration of various forms of inorganic nitrogen had largely positive linear
438 responses to BLs and PCs in both the surface and subsurface, with strongly negative responses in PGs and subsurface MGDGs.
439 Among the SQDGs, many individual molecular species, with different fatty acid chains, responded linearly to all forms of
440 inorganic N, the signs of these relationships were negative but, in the surface, and generally positive in the subsurface (aside
441 from NO_2^-). DGDGs showed only one positive linear response in the subsurface. PEs showed little response to inorganic
442 nitrogen concentrations (regression coefficients near 0). PO_4^{3-} concentrations showed only a few significant responses from
443 BLs (negative) and PGs (slightly positive) in the surface. However, in the subsurface, PO_4^{3-} showed strong linear responses
444 (negative) to several MGDG and PG molecules, and strong positive relationships with several PCs.

445

446 Light showed few linear responses amongst IPL relative abundances. At the surface, the strongest relationships were amongst
447 PG (positive) and SQDG (mixed signs) and to a slight degree BLs (negative). In the subsurface, only one SQDG with a
448 significant linear relationship was noted and with a weak regression coefficient, indicating a range of light saturation with little
449 to no linear effect on IPL distributions.

450

451 **3.7 CART and Random Forest**

452 All the predictive tree-based models showed improved performance with the inclusion of environmental variables (Figs. 4-7).
453 The CART decision trees iteratively identified the key biological and physicochemical variables producing the best performing
454 model in the prediction of IPL concentrations. The random forest analysis compliments these best fit decision trees by
455 calculating the % reduction in the root mean square error (RMSE) associated with each variable. In conjunction, these two
456 analyses highlight the most impactful variables in predicting the concentrations of a given IPL class. Overall, model
457 performance amongst each IPL class can be compared by the strength of the correlation coefficients between observed and
458 predicted concentrations, and by the magnitude of the RMSE (Figs. 4-7).

459

460 Amongst several IPL classes (i.e., SQDGs, DGDGs, and BLs), pH_T was consistently a significant contributing variable to IPL
461 concentrations, as demonstrated by both the CART and random forest analyses (Fig. 4A-D, and Fig. 5). Notably, pH_T was
462 identified as the most important variable amongst the best fit decision trees for both SQDGs and DGDGs, as well as the random
463 forest model for SQDGs. Oxygen concentration was also frequently identified as a major contributing variable to model
464 performance with MGDGs, DGDGs, PEs, PCs, (Figs. 4E-H, 5A-D, 6E-H, and 7A-D, respectively) and moderately important

465 in SQDGs (Fig. 4A-D). Temperature was selected as the most important variable in PE predictions (Fig. 6E-H), and a major
466 contributing variable in SQDG, MGDG, BL, PG, and PC predictions (Figs. 4-7). Various forms of biologically available
467 nitrogen were also important in the prediction of MGDG (Figs. 4E-H), BLs (NH_4^+ ; Figs. 5E-H), PE (NH_4^+ ; Figs. 6E-H), and
468 PG (NH_4^+ and NO_2^- ; Figs. 6A-D). PO_4^{3-} concentrations showed significant contribution to model performance amongst BLs
469 (Figs. 5E-H, denoted as Si:P ratios), SQDGs, MGDGs, PGs, and PEs (Figs. 4A-D, 4E-H, 6A-D, and 6E-H, respectively).
470 Finally, light availability demonstrated secondary but significant importance in the prediction of SQDGs, MGDGs, PGs, PEs,
471 and PCs (Figs., 4A-D, 4E-H, 6A-D, 6E-H, and 7 respectively).

472

473 Variables indicative of biological abundance were also identified as highly impactful to model performance, with chl-a
474 concentration showing a significant contribution to all lipid classes except BLs (Figs. 4-7). Individual phytoplankton
475 abundances also showed to be important predictive variables such as Cryptophyceae abundances for BLs, dinoflagellate
476 abundances for DGDGs and SQDGs, *Synechococcus* abundances for DGDGs, PCs, PEs, and PGs, and diatoms for PCs.

477 **3.8 Water Treatments**

478 The experiment consisted of applying two different treatments to the mesocosms, aimed at exploring the varying impacts of
479 upwelling of ODZ waters with contrasting geochemical properties. The first treatment saw the introduction of water from a
480 coastal area (station 1) with ODZ waters with a very low N:P ratio (0.1; see Table 1, and Fig 2B) into the mesocosm. The
481 second treatment performed the same process, but with ODZ water from an offshore area (station 3) with a low N:P ratio (1.7;
482 Table 1, and Fig 2B). Despite the different chemical signatures of the added water-masses, the resulting nutrient stoichiometries
483 within the mesocosms were similar in between both treatments, likely due to both dilution effects and the time passed between
484 water collection and addition (see Bach et al., 2020). We see largely similar responses in the IPL distributions, as well as in
485 other biogeochemical variables between these two treatments; therefore, we largely focus our discussion on the temporal
486 variation and differences between surface and subsurface environments in these analyses.

487 **4 Discussion**

488 **4.1 Biological Abundances as Drivers of IPL Distributions**

489 We expect phytoplankton abundances to exert first order control on the production and distribution of IPLs in this experiment.
490 The majority of the detected molecules have been demonstrated to be chemotaxonomic biomarkers of planktonic biomass
491 (Sturt et al., 2004, Schubotz et al., 2009, Wakeham et al., 2012; Van Mooy and Fredricks, 2010; Cantarero et al., 2020).
492 Previous work in the Humboldt Current System shows that the ratio of total IPLs to POC is high at the chlorophyll maximum
493 and the composition of IPLs found in these surface waters are consistent with predominantly phytoplanktonic biomass
494 (Cantarero et al., 2020). In this mesocosm experiment, the depths of the chlorophyll maximum and oxycline are compressed
495 into a 20 m water column which likely drives a greater contribution of phytoplanktonic IPLs in ODZ waters than would be

496 expected in the natural environment. While we suggest that most of the biomass (and IPL content) measured at these high
497 chlorophyll depths is likely derived from phytoplankton, we cannot completely isolate nor quantify the contribution of bacterial
498 biomass to the total IPL pool.

499
500 Most IPL classes demonstrate phytoplankton abundances as a primary or major predictor in the CART and random forest
501 analyses, such as dinoflagellates in the prediction of SQDGs (Figs. 4A, C), DGDGs (Figs. 5A, C), and PE (Fig. 6G),
502 *Synechococcus* in the prediction of PGs (Fig. 6A, C), PEs (Fig. 6E, G), and PCs (Fig. 7A, C), and chl-a in the prediction of
503 every IPL class barring BLs (a mostly minor IPL class in this experiment). Chl-a appears most important in highly abundant
504 IPL classes as an indicator of overall photosynthetic productivity, and dinoflagellates dominate the overall phytoplankton
505 biomass for almost the entirety of the experiment post ODZ water addition. *Synechococcus* demonstrates covariance with the
506 total phytoplankton biomass, yet remains a relatively minor phytoplankton class. We suggest that the prevalence of biological
507 sources as IPL predictors in the decision tree analyses generally indicates the variability in total phytoplankton biomass
508 throughout the experiment.

509
510 Among phytoplankton, glycolipids MGDG, DGDG, and SQDG are predominantly found in thylakoid membranes, whereas
511 phospholipids PC and PE, as well as BLs are structural components in the cell membrane lipid bilayer (note PG is found in
512 both; Guschina and Harwood, 2013). It is important to recognize that the relative proportions of IPLs vary in different
513 phytoplankton classes (Harwood and Jones, 1989; Wada and Murata, 2009), and that many of these lipids, in particular
514 phospholipids, can also be derived from heterotrophic bacterial biomass (Popendorf et al., 2011). Thus, the overall community
515 composition is expected to be a major driver of IPL distributions in this system. However, given the prevalence of algal biomass
516 and the steps taken to minimize bacterial contributions to the IPL pool (see section 2.5), we focus our analysis on that of
517 phytoplanktonic dynamics. We recognize that both phytoplankton abundances and the total planktonic community
518 composition play a major role in the distribution of IPLs. Thus, while the data presented here may refine the phylogenetic
519 association between biological sources and IPLs in marine systems, our main aim is to explore the role of multiple
520 environmental forcing as an additional control on IPL distributions. The following sections focus on the evidence for direct
521 environmental influence on IPL remodeling amongst the phytoplankton community and the potential implications of these
522 physiological responses to broader aspects of ocean biogeochemistry.

523 **4.2 Environmental Variables as Drivers of IPL Remodeling**

524 Since community composition can change concurrently and/or in response to environmental conditions, we employed two
525 distinct strategies to isolate the role of lipid remodeling as a physiological response to environmental forcing only. Firstly, the
526 MLRs which subtract the variability explained by phytoplankton abundance (e.g., CHEMTAX results) in pairwise correlations
527 between lipid abundances and environmental variables. Secondly, the decision tree analyses (CART and Random Forest)
528 which rank variables by their impacts on the model performance.

529

530 Across virtually every major IPL class common to eukaryotic phytoplankton we see evidence of environmental conditions
531 exerting significant control on polar headgroup distributions in the MLRs (Fig. 3). Similarly, nutrient concentrations, pH_T,
532 temperature, O₂ concentration, and light availability are consistently identified as statistically important variables in the
533 prediction of IPL head groups in both the CART and Random Forest analyses (Figs. 4-7). In addition, high level comparisons
534 in the relative abundances of IPLs and phytoplankton groups (Figs. 3C, D) suggest that certain environmental conditions may
535 be associated with major shifts in IPL distributions.

536

537 An important distinction between the MLRs and the decision trees is that the MLRs are calculated within individual depth
538 environments (surface and subsurface) to explore statistically significant linear relationships between abundant IPL molecules
539 and changing environmental conditions. On the other hand, the decision trees explore the predictive power of physicochemical
540 differences between the surface and subsurface environments on IPL distributions. The results of these two analyses are meant
541 to be complimentary, in that they focus on the differences in environmental conditions between water depths as well as the
542 temporal development of conditions within a given depth over the course of the experiment.

543 **4.2.1 Nutrient Availability**

544 Nutrient limitation amongst phytoplankton leads to transitions in cellular activity, from the biosynthesis of
545 growth/reproduction cellular components such as cell membranes to energy storing molecules (Guschina and Harwood, 2013,
546 Zienkiewicz et al., 2016). Nitrogen, an essential nutrient in photosynthesis and the biosynthesis of proteins/enzymes and
547 nucleic acids, is typically acquired by marine phytoplankton through inorganic nitrogen species such as NO₃⁻ and NH₄⁺. Some
548 phytoplankton can also utilize organic nitrogen sources (Bronk et al., 2007), whereas diazotrophic cyanobacteria can fix
549 dinitrogen gas into bioavailable nitrogen. The coastal region of the ETSP is typically considered to be seasonally co-limited
550 by light, N, and Fe (Messié and Chavez, 2015). However, along the Peruvian shelf Fe concentrations are elevated compared
551 to offshore waters (Hutchins et al., 2002; Browning et al., 2018), and is not considered a limiting source in this mesocosm
552 experiment (Bach et al., 2020). In our mesocosm systems, the inorganic N:P ratio ranged between 0.13 and 4.67, with higher
553 inorganic N in subsurface waters compared to the surface, and with a N:P minimum reached by day 20. Bach et al., (2020)
554 noted that a week after the ODZ water addition, increases in the particulate organic carbon to biogenic silica ratios coincided
555 with low inorganic N and high Si(OH)₄ concentrations, suggesting a N-limited system. Thus, we consider our system to be
556 overall nitrogen limited with varying degrees of severity throughout the course of the experiment. This N-limitation is also
557 reflected in the transition from predominantly diatoms, Chlorophyceae, and Cryptophyceae to a dominance of mixotrophic
558 dinoflagellates approximately 4-6 days after the initial ODZ water treatment (Bach et al., 2020). Such shifts are consistent with
559 the ecological advantage that dinoflagellates exhibit under N-limiting conditions as they can extract nitrogen from the dissolved
560 organic nitrogen (DON) pool (Kudela et al., 2010) as well as from heterotrophy (Smalley et al., 2003).

561

562 In our study, all four mesocosms experienced limitations in inorganic nitrogen (as low as 0.24 $\mu\text{mol/L}$) and consistently high
563 concentrations of PO_4^{3-} (ranging from 1.3 to 2.3 $\mu\text{mol/L}$) throughout the entire experiment. Random forest analysis shows that
564 the inorganic N concentration is an important predictor in the abundance of BL, PG, and MGDG (Figs. 5G, 6A, and 4E,
565 respectively). The MLRs also indicate that many individual molecules from nearly every IPL headgroup have significant linear
566 correlations with inorganic N concentrations (Fig. 3). Of note, the distributions of several abundant PCs and BLs with N in the
567 headgroup structure are consistently positively correlated with inorganic N species. Whereas other non-N-bearing IPLs are
568 generally negatively correlated with inorganic N concentration (PG, SQDG and MGDG) meaning that they are proportionally
569 more abundant under more severe N-limitation.

570

571 Under P limitation, phytoplankton are known to substitute non-phosphorus-containing glycolipids for phospholipids and
572 reallocate the liberated P for other cellular demands (Van Mooy et al., 2009). We hypothesize that non-N-containing
573 glycolipids and phospholipids may similarly be substituted for IPLs such as PCs and BLs as a mechanism for alleviating
574 cellular N demand in low inorganic N conditions. Both PC and BL are found in extra-chloroplast membranes (Kumari et al.,
575 2013), whereas IPLs found in thylakoid membranes such as MGDG, PG, and SQDG are essential to the photosynthetic
576 machinery. Indeed, the average ratio of total IPLs/chl-a is up to three times higher at depth than in surface waters (Fig. S5),
577 possibly pointing towards a reduced proportion of membrane lipids among phytoplankton subject to environmental stressors
578 such as nutrient limitation (likely in addition to oxygen availability, temperature, and light levels). We note that at least a
579 fraction of this trend could also be explained by the contribution of IPLs from heterotrophic bacteria.

580

581 More generally, nutrient limitation can cause phytoplankton to accumulate highly concentrated stores of energy in the form of
582 triacylglycerols (TAGs) through the activation of multiple biosynthetic pathways (Zienkiewicz et al., 2016). These include
583 synthesis via acyl units donated from phospholipids via the PDAT (phospholipid:diacylglyceroltransferase) enzyme (Dahlqvist
584 et al., 2000), or other chloroplast membranes, as demonstrated in the homologous enzyme Cr-PDAT (Yoon et al., 2012), as
585 well as several DGAT(diacylglycerol:acyl-CoA acyltransferases; Li et al., 2012; Li-Beisson et al., 2019). These enzymes
586 represent significant pathways for TAG accumulation (Popko et al., 2016; Gu et al., 2021), are sensitive to N availability
587 (Yoon et al., 2012; Li et al., 2012), and their encoding genes have so far been identified in green algae, diatoms, and heterokonts
588 (Zienkiewicz et al. 2016). Because our dataset does not include TAG production, further work on this aspect could reveal
589 whether the proportional changes in dominant phytoplanktonic IPLs correlated to N availability are also associated with TAG
590 synthesis, and if so, determine whether recycling of membrane lipids is a significant contributor to these observed community-
591 level distributions.

592

593

594 4.2.2 pH_T and Inorganic Carbon Availability

595 Coastal upwelling zones are characterized by low pH_T subsurface waters associated with ODZs, where high fluxes of organic
596 substrates sustain enhanced microbial respiration and the accumulation of CO₂ (Capone and Hutchins, 2013). Thus, we explore
597 evidence for membrane lipid remodeling amongst phytoplankton as a physiological response to varying pH_T. We see evidence
598 of pH_T imparting a potential control on the composition of IPL head groups, particularly amongst SQDGs and DGDGs, as
599 noted by the high importance rankings in both the CART and Random Forest analyses (Figs. 4A,C and 5A,C). This likely
600 represents the relatively high abundance of these glycolipids in the surface samples where the pH_T is 0.2-0.6 higher than at
601 depth. The MLRs show several negative correlations between MGDG, PG, and SQDG molecules containing unsaturated or
602 polyunsaturated fatty acids with pH_T (Fig. 3). The observed increased proportion of unsaturated IPLs at lower pH_T is most
603 apparent in surface waters where the variability in pH_T is greatest (± 0.2). It has been suggested that lower pH_T can induce
604 greater proportions of saturated fatty acids as a mechanism to reduce membrane fluidity and prevent high proton concentrations
605 in the cytoplasm (Tatsuzawa et al., 1996). However, this response remains limited to more extreme pH_T ranges (e.g., ~1-10),
606 suggesting that other environmental factors (e.g. nutrient availability) are overprinting the potential impacts of pH on fatty
607 acid saturation.

608
609 Rather than a direct consequence of modest changes in pH_T on algal membrane fluidity, the observed changes in fatty acid
610 profiles may be in part a response to the available forms of inorganic carbon for photosynthesis. Following the ODZ water
611 addition, DIC (dissolved inorganic carbon) and pCO₂ rapidly declined within a few days (Chen et al., 2022) due to high
612 productivity. In natural waters, pCO₂ maxima occur in ODZ waters where respiration rates are high (Vargas et al., 2021).
613 Lower pCO₂ at the surface may be a limiting factor for photosynthesis and growth; higher pH_T in marine settings indicates a
614 reliance on active transport of HCO₃⁻ for carbon fixation as opposed to a passive diffusion of CO₂ (Azov et al., 1982; Moazami-
615 Goudarzi et al., 2012). Enrichment of pCO₂ has also been observed to induce an increased proportion of unsaturated fatty acids
616 in microalgae (Morales et al., 2021), which may explain the negative correlation between the proportion of certain unsaturated
617 glycolipids (as well as PGs) and pH_T (high pCO₂; see Fig. 3).

618
619 As mentioned above, phytoplankton can employ membrane lipids as substrates for TAG accumulation in phytoplankton under
620 environmental stress. While nutrient limitation is often considered the primary regulator of TAG production, culture
621 experiments also point toward the importance of pH and inorganic carbon availability (Guckert and Cooksey, 1990; Gardner
622 et al., 2011), with different responses between a model diatom (*Phaeodactylum tricornerutum*) and chlorophytes (CHLOR1 and
623 *Scenedesmus sp.* WC-1), which is potentially related to individual carbon concentrating mechanisms (Gardner et al., 2012).
624 For instance, under nitrogen/phosphorus limitation, TAG production can be promoted if the supply of inorganic carbon is
625 abundant (Peng et al., 2014). TAGs can also be synthesized and accumulated when inorganic carbon is limited by invoking
626 the recycling of IPLs such as glycolipids and phospholipids (Peng et al., 2014). Thus, the higher proportions of SQDGs and

627 DGDGs in the high pH/low CO₂(aq) surface waters of our experiment could be in part related to their recycling under CO₂
628 limitation.

629

630 Overall, our results are consistent with other experimental data in that pH_T impacts the distribution of IPL head groups amongst
631 certain phytoplankton groups. For instance, the relatively high glycolipid abundances in surface samples with higher pH_T (most
632 notably SQDG and DGDG, see Fig. S1) are likely not related to direct effects on membrane fluidity, but rather to the
633 availability of inorganic carbon and its effect on the recycling of phospholipids (as well as MGDGs), potentially for TAG
634 synthesis. While our results are consistent with the so far observed IPL substrates for TAG synthesis (Dahlqvist et al., 2000;
635 Yoon et al., 2012), additional analyses of TAG concentration and their fatty acid compositions amongst the phytoplanktonic
636 community would aid in tracing the extent of membrane lipid degradation as a source of acyl units, as well as to trace the
637 location of these biosynthetic pathways in the cell. Such work would aid in determining the extent to which TAG synthesis
638 and IPL recycling relegates phytoplankton classes to certain depths of the water column based on the combined effects of
639 nutrient availability and pH_T (amongst other variables; e.g. light, temperature, O₂.)

640

641 **4.2.3 Oxygen**

642 Despite the harvesting of light energy during photosynthesis, photosynthetic organisms also rely on respiration for growth and
643 free radical scavenging under both light and dark conditions (Raven and Beardall, 2003). Specifically, the availability of O₂
644 (particularly during the dark phases or in low-light environments) influences the activation of metabolic responses, such as
645 fermentative metabolism and acetate utilization (Yang et al., 2015). Differences in dark respiration rates relative to light-
646 saturated photosynthesis among algae may confer advantages under varying oxygen availability (Geider and Osborne, 1989).
647 Thus, the ability of some organisms to perform lipid remodeling in response to oxygen stress may partially shape the
648 composition of the phytoplankton community.

649

650 In our analysis, the Random Forest models indicate a significant impact of O₂ concentration in the prediction of nearly all IPL
651 class abundances (Figs. 4-7). This pattern appears to be largely driven by differences in IPL distributions between surface
652 (oxygenated) and subsurface (hypoxic; < ~1.4 ml/L as defined by Naqvi et al., 2010) waters. Glycolipids (MGDG, DGDG,
653 and SQDG) make up on average 28% more of the IPL pool in the oxygenated surface waters (~125-220 μmol/L O₂) compared
654 to oxygen deficient subsurface waters (~15-75 μmol/L O₂). The MLRs, however, show no significant relationships between
655 individual glycolipid relative abundances and O₂ concentration in surface samples (Fig. 3); this is possibly due to surface
656 waters remaining well oxygenated throughout the experiment. While several IPL moieties found in BLs, SQDGs, and PGs
657 demonstrate mostly negative linear relationships (Fig. 3), we suggest that the most prominent and consistent relationships are
658 driven by a major shift from oxic to hypoxic conditions (i.e., surface vs subsurface) as opposed to a sensitivity to variable O₂
659 concentrations.

660

661 Anaerobiosis amongst green algae has been demonstrated to impact lipid production, with significant reductions (by nearly
662 50%) in polar lipid content and concomitant increases in fatty acids (Singh and Kumar, 1992). Gombos and Murata (1991)
663 found that the cyanobacterium *Prochlorothrix hollandica* experienced a significant reduction in the relative abundance of
664 MGDGs that coincided with moderate increases in SQDGs, DGDGs, and PGs under low oxygen conditions. Furthermore,
665 culture experiments of anaerobically grown *Chlamydomonas reinhardtii* resulted in both decreased membrane lipid yields
666 (most notably amongst MGDGs and DGDGs; by > 50%) and an accumulation of TAGs (Hemschemeier et al., 2013). It has
667 been noted that oxygen stress appears to induce the degradation of fatty acids (~30% reduction under dark/anaerobic
668 conditions), mostly amongst unsaturated fatty acids commonly found in MGDG and DGDG membrane lipids (16:4 and 18:3)
669 used for TAG assembly (Liu, 2014; Hemschemeier et al., 2013). Glycolipids (i.e., MGDG and DGDG) appear to serve as
670 important substrates for TAG production under low oxygen conditions; however, beta-oxidation of fatty acids requires oxygen
671 to contribute to the degradation of acyl groups, potentially explaining why membrane lipid degradation is attenuated under
672 more severe hypoxia (Liu, 2014). This physiological response to low oxygen conditions in subsurface waters may explain the
673 relatively high abundance of glycolipids in well oxygenated surface waters.

674

675 Dinoflagellates have been shown to exhibit particularly high dark respiration to light-saturated photosynthetic rates as
676 compared to diatoms, Chlorophyceae, or most notably cyanobacteria (Geider and Osborne, 1989), possibly pointing towards
677 a greater sensitivity to O₂ concentrations. In addition to other environmental conditions, the greater relative abundance of
678 Chlorophyceae, diatoms, and Cryptophyceae in the oxygen-deficient subsurface waters may reflect reduced respiration rates
679 amongst these algae. Differences in the proportion of glycolipids MGDG and DGDG amongst different algae, and their relative
680 ability to recycle them under oxygen stress, may play a prominent role in their individual tolerances to oxygen limitation.

681

682 Higher proportions of glycolipids in surface waters may also be due to enhanced rates of microbial degradation under oxic
683 conditions, which may be 2-4 times faster than under anoxic conditions, as tested in microcosm experiments (Ding and Sun,
684 2005). Relatively labile glycolipids can accumulate in the dissolved organic carbon pool (Gašparović et al., 2013). This
685 observation aligns with the slower breakdown of SQDGs compared to phospholipids observed in IPL degradation experiments
686 under aerobic conditions (Brandsma, 2011). This accumulation process, however, is unlikely in regions of the water column
687 with large numbers of active living cells, and highly active bacterial degradation. In fact, the distributions of IPLs across the
688 ODZ of the ETSP indicate minor contributions of exported IPLs to greater depths, suggesting high surface recycling (Cantarero
689 et al., 2020). However, specific experimental observations encompassing oxygen gradients ranging from well-oxygenated to
690 fully anoxic conditions are necessary to derive more robust conclusions.

691

692 4.2.4 Temperature

693 Phytoplankton have been shown to respond variably to high growth temperatures depending on their individual tolerances
694 (Huertas et al., 2011). Photosynthesis is considered the most heat-sensitive cellular function in photoautotrophs (Berry and
695 Björkman, 1980). In this section we discuss the potential lipidomic responses to heat stress within the IPL distributions of the
696 phytoplanktonic community. Temperature fluctuations affect membrane fluidity, a phenomenon commonly controlled by fatty
697 acid desaturases (Sakamoto and Murata 2002) that catalyze the production of unsaturated/saturated fatty acids to
698 increase/decrease membrane fluidity, respectively (Lyon and Mock 2014). We did not see evidence for temperature effects on
699 the degree of unsaturation in our data (see Fig. S2). This is likely due to the overall narrow temperature range observed during
700 the experiment (17.3 - 21.6 °C), which mirrors the natural variability observed in Callao (average monthly ranges ~16.6-19.6
701 °C from 2017 to 2019 (Masuda et al., 2023).

702
703 Despite the restricted temperature range and its lack of impact on the unsaturation degree of core lipids, the random forest
704 analyses identified temperature as a significant variable in predicting all IPL classes based on their polar head groups aside
705 from DGDG and PE (Figs. 4-7). This suggests that the response to temperature may vary among different IPLs classes. The
706 MLRs indicate consistently positive relationships between several glycolipids and temperature, suggesting a potential
707 physiological compensation via membrane compositions for higher temperatures. Gašparović et al. (2013) noted an
708 accumulation of glycolipids at temperatures >19 °C in the northern Adriatic Sea, particularly from cyanobacterial synthesis of
709 MGDGs. The sensitivity of photoautotrophs to thermal stress was also explored by Yang et al. (2006), who showed that
710 DGDGs and MGDGs both increase the thermal stability of photosystem II, while phospholipids significantly decrease it.
711 Experiments with a wild-type and mutant *Chlamydomonas reinhardtii* have shown that SQDGs are an essential component of
712 thylakoid membranes to maintain stability under heat stress (Sato et al., 2003), although at considerably more extreme
713 temperatures (41 °C). Heat stress has also been linked to the production of TAGs (Elsayed et al., 2017; Fakhry and El
714 Maghraby, 2015), which can draw acyl units from degraded membrane lipids (Holm et al., 2022).

715
716 Interestingly, the relative abundance of DGDGs in our experiment shows the most prominent (R^2 of 0.35-0.44), and statistically
717 significant ($p < 0.05$), linear relationship with temperature (see Fig. S3A). While temperature was not identified as an important
718 variable to the prediction of DGDGs in either decision tree analysis, this may be due to other covariates, such as pH and O_2 ,
719 masking the effect of temperature. Our results indicate that phytoplankton may either produce DGDGs in greater abundance
720 to alleviate thermal instability in photosystem II, or preferentially degrade other thylakoid membranes (i.e., PGs, SQDGs, or
721 MGDGs) in response to heat stress, leaving the remaining IPL pool relatively enriched in DGDGs. While several individual
722 MGDG and SQDG molecules did demonstrate linear responses to temperature (Fig. 3), other stressors such as N availability,
723 pH, and light levels may confound the effects of temperature in the overall abundance of these lipid classes.

724 4.2.5 Light Availability

725 Bach et al. (2020) considered the overall productivity in these mesocosm experiments to be co-limited by N and light
726 availability, which have been identified as key limiting factors in eastern boundary upwelling systems (Messié and Chavez,
727 2015). In our experiment, initial high biomass productivity led to self-shading effects that significantly reduced the PAR (Bach
728 et al., 2020). While the maximum photon flux densities measured at noon over the course of the experiment were $\sim 500 - 600$
729 $\mu\text{mol m}^{-2}\text{s}^{-1}$, only $\sim 5-22\%$ and $< 4\%$ were measured in surface (~ 2 m) and subsurface (17 m) waters, respectively, from all four
730 mesocosms. While both depth-integrated samples in our experiment are likely from light-limited planktonic communities,
731 most PAR values ($> 15\%$ i.e., $75-132 \mu\text{mol m}^{-2}\text{s}^{-1}$) in surface waters still demonstrate sufficiently high levels that can affect
732 lipid production and accumulation (Gonçalves et al., 2013) especially under the combined effects of N-deprivation (Yeesang
733 and Cheirsilp, 2011; Jiang et al., 2011).

734
735 Light levels are identified by the Random Forest analyses to be a significant variable in the prediction of MGDGs, SQDGs,
736 PGs, and PCs (Figs. 4, 6, and 7). While few studies have explored the direct effects of irradiance levels on IPL headgroup
737 distributions, experimental cultures of *Tichocarpus crinitus* found increased IPL production of SQDGs, PGs, and PCs amongst
738 shade-grown algae (Khotimchenko and Yakovleva, 2005). In *Tichocarpus crinitus* cultures, MGDGs, one of the most abundant
739 thylakoid lipids, show decreased abundances under low light conditions (Khotimchenko and Yakovleva, 2005). Our results
740 show that both MGDGs and SQDGs are present in greater relative and absolute abundances in the surface waters where light
741 is less limited or potentially inhibitive at times, suggesting an impact on thylakoid lipid compositions to maintain efficient
742 photosynthetic rates under changing light conditions. MGDGs have been shown to provide important photoprotective and
743 antioxidant mechanisms in diatoms (Wilhelm et al., 2014), potentially explaining their higher abundance in the surface waters
744 and the significance of light in the Random Forest models. While the exact function of SQDGs in thylakoid membranes remains
745 unclear, they have been observed to act as an antagonist to the aggregating action of MGDGs (Goss et al., 2009), leading to a
746 disaggregating effect on light harvesting complexes (Wilhelm et al., 2014). The latter potentially reflects planktonic responses
747 to variable PAR (5-22%) in the surface via adjustment of the proportions of SQDGs and MGDGs in the thylakoids (Gabruk et
748 al., 2017; Nakajima et al., 2018).

749
750 The PC lipid class, primarily found in extrachloroplast membranes (Mimouni et al., 2018), consistently exhibits greater relative
751 abundance in the subsurface compared to surface waters. We suggest that light levels at depth may play a role (albeit a
752 secondary one, see Fig. S3B) in non-chloroplast IPL production when algal cells are configured for rapid growth/reproduction.
753 Conversely, under higher light as well as under the combined effects of DIC and N limitation at the surface, algal cells are
754 more prone to survival responses such as TAG production at the expense of IPLs. PG can be found in extrachloroplast
755 membranes but is also an essential component of photosystems I and II, with important roles in electron transport processes
756 (Sakurai et al., 2003; Wada and Murata, 2009; Kobayashi et al., 2017). The overall abundance of PGs contributing to the total

757 IPL pool may be influenced by varying production of certain non-chloroplast membranes under lower light conditions, and
758 other thylakoid membranes under high light conditions, thus possibly explaining the highly variable overall contribution of
759 PGs to the IPL pool. Additional analyses of specific fatty acid structures from intact PGs may illuminate sources within the
760 cell, i.e., thylakoid PGs and extrachloroplastic PGs.

761
762 Light intensity has also been shown to have contradictory impacts on fatty acid composition, with some analyses observing
763 increased unsaturation under high light intensity (Liu et al., 2012; Pal et al., 2011). Others observed that excess light energy
764 induces synthesis of saturated (SFAs) or monounsaturated (MUFAs) fatty acids in several algal species to prevent
765 photochemical damage, or the synthesis of polyunsaturated fatty acids (PUFA) for the maintenance of photosynthetic
766 membranes under low light conditions (Khoeyi et al., 2012, Fabregas et al., 2004, Sukenik et al., 1993; Orcutt and Patterson,
767 1974). However, we see limited evidence in this experiment of a direct correlation between light intensities and fatty acid
768 composition in the multiple linear regressions (Fig. 3). This may be related to differences in optimal irradiance levels between
769 algal groups overlapping to confound any clear patterns.

770
771 Given that the normalized PAR in surface waters remains <25%, and that light appears as a variable of significant but secondary
772 importance in the random forest models, our results suggest that under these experimental conditions, low or variable light
773 availability may amplify the effects of other environmental stressors (i.e., nitrogen availability, oxygen concentration,
774 temperature, and inorganic carbon availability). The effects of self-shading from high biomass production early in the
775 experiment, when greater nutrient availability was high, likely contributed to the markedly different IPL distributions observed
776 between surface and subsurface waters. As a result, the fluctuations in PAR may play a role in the observed variations in the
777 relative proportions of prevalent thylakoid membrane IPLs, including MGDGs, SQDGs, and PGs.

778 779 **4.3 Implications of IPL Remodeling in Phytoplankton Membranes**

780 We expect the ongoing changing conditions in the ETSP, such as rising temperatures, ocean acidification, expanding ODZs,
781 and shifts in upwelling-driven nutrient supply, to instigate multiple physiological responses amongst phytoplankton
782 communities. IPL remodeling and the reallocation of resources among algae are likely to have cascading effects on the
783 composition of phytoplanktonic communities, the nutritional value of algal biomass to higher trophic levels, and the cycling
784 of organic carbon and nitrogen in the upper ocean. Here, we explore the potential consequences of these physiological
785 responses to environmental conditions and outline future areas of investigation to better constrain the impacts of IPL
786 remodeling on marine biogeochemistry.

787

788 4.3.1 Relative adaptability of Phytoplankton Classes to environmental change

789 IPL classes are either partitioned to the thylakoid membranes (i.e., MGDG, DGDG, SQDG, and PG) in variable distributions
790 to maintain photosynthetic function, or to extraplastidic membranes under growth/reproductive phases (BL, PC, PE, and PG).
791 As environmental conditions change, the ability of phytoplankton to adjust these IPL compositions may be an important driver
792 controlling the phytoplankton community structure. Within a few days of the ODZ water addition, the mesocosms became
793 oligotrophic, which coincided with a major shift in phytoplankton groups, from predominantly diatoms, Chlorophyceae, and
794 Cryptophyceae to a dominance of ‘survivalist’ mixotrophic dinoflagellates. An obvious advantage of mixotrophic
795 dinoflagellates to the largely N-limited conditions of this experiment is their ability to extract N from the DON pool, and a
796 lower dependence on light compared to the other previously mentioned phytoplankton groups.

797
798 To contextualize the impacts of IPL remodeling on the phytoplanktonic community, we performed an additional random forest
799 analysis to identify the most important IPLs (both individual moieties and polar head group totals) in the prediction of
800 individual phytoplankton classes. We applied this analysis to identify what IPL remodeling processes may be more readily
801 available to each major phytoplankton class in this experiment (Fig. 8). While all the phytoplankton classes are likely to
802 produce each IPL class to varying extents, the differences in their relative distributions may provide insight into differences in
803 phytoplankton adaptability under changing environmental conditions. Dinoflagellates are heavily associated with high
804 abundances of the glycolipids SQDG and DGDG, with far less apparent dependence on phospholipids and MGDGs (Fig. 8).
805 The dominance of dinoflagellate biomass is attributed to the severe scarcity of inorganic nitrogen and relatively low light
806 intensity due to self-shading effects (Bach et al., 2020). Dinoflagellates may also take advantage of the recycling of N-bearing
807 PCs and BLs to alleviate nitrogen limitation or to produce energy storing TAGs. The high proportion of DGDGs and SQDGs
808 and recycling of MGDGs may also prove advantageous under high pH/low pCO₂ conditions in surface waters, alleviating pH
809 stressors, or the energy investment in active HCO₃⁻ transport for photosynthesis. These IPL remodeling strategies may have
810 played a role in the dominance of dinoflagellates under the post-upwelling experimental conditions.

811
812 In the early phases of the experiment and when inorganic N is readily available, diatoms (and to a lesser extent Cryptophyceae
813 and Chlorophyceae) dominate the water column biomass. Each of these phytoplankton classes (as well as *Synechococcus*)
814 indicates a greater dependence of the N-bearing PCs and/or BLs, potentially signaling a reduced capacity to scavenge these
815 extrachloroplastic IPLs within the cell for N, or as substrates for TAG production. Notably, these phytoplankton consistently
816 make up a greater proportion of the total chl-a pool in subsurface waters, suggesting an ability to accommodate the lower O₂
817 concentrations and pH in exchange for greater N availability (see summary in Fig. 8). Some of this adaptability may be related
818 to the recycling of MGDGs for additional acyl units under hypoxia (most likely amongst Chlorophyceae and *Synechococcus*),
819 and/or the generally higher relative production of structural membrane lipids under low light growth conditions (see impact of
820 light discussion above).

821

822 In the Eastern Tropical South Pacific (ETSP), upwelling events exhibit a distinctive trend of increasing frequency and intensity,
823 setting it apart from other eastern boundary systems (Abrahams et al., 2021; Oyarzún and Brierley, 2019). This phenomenon
824 brings about important changes in environmental conditions, including a decrease in sea surface temperature ($\sim 0.37^{\circ}\text{C}$, average
825 from 1982 to 2019, Abrahams et al., 2021) alongside oxygen reduction and reduced pH in the coastal zones of the region
826 (Pitcher et al., 2021). Simultaneously, there is an observed boost in primary productivity (Gutierrez et al., 2011; Tretkoff,
827 2011). The impact of strong upwelling, followed by rapid thermal stratification when upwelling subsides, could signify abrupt
828 changes that affect the community structure of phytoplankton (Gutierrez et al., 2011). Such environmental changes favor
829 species better adapted to stress conditions, such as mixotrophic dinoflagellates and silicoflagellates, at the expense of diatom
830 populations (Hallegraeff, 2010), which could translate to a decrease in highly nutritious saturated fatty acids for higher trophic
831 levels (Haus et al., 2012). Furthermore, a potential reduction in diatom biomass and diversity could have consequences on
832 the ocean biological carbon pump (Tréguer et al., 2018).

833

834 Under the ongoing and projected scenarios of climate change, our mesocosm experiment demonstrates how shifts in the
835 phytoplankton community translate into changes in the lipid composition of their cell membranes. This adds weight to the
836 school of thought that lipid remodeling amongst the phytoplankton community could have repercussions at higher trophic
837 levels, as recently discussed by Holm et al. (2022), and on ocean biogeochemistry as we discuss below.

838

839 **4.3.2 Cycling of Carbon, Nitrogen, and Sulfur**

840 Combined, neutral (TAGs) and polar lipids (IPLs) make up on the order of 17.6% to 34.7% of the cell by dry weight under N-
841 replete and N-deprived conditions, respectively (Morales et al., 2021), with other environmental stressors able to compound
842 the accumulation of neutral lipids (Zienkiewicz et al., 2016). This represents a considerable portion of algal cellular carbon,
843 and total water column carbon stocks that supply the transfer of fatty acids to higher trophic levels (Twining et al., 2020).
844 Trophic transfer of fatty acids to grazing zooplankton may be affected by the relative contribution of polar and neutral lipids,
845 as they can have significantly different turnover rates (Burian et al., 2020). This suggests that the relative concentrations of
846 TAGs/IPLs in phytoplanktonic communities may impact the rates of fatty acid remineralization or uptake into higher trophic
847 levels. Additionally, while our analysis did not focus on individual fatty acid structures, other experiments investigating the
848 effects of increasing $p\text{CO}_2$ and nitrogen deficiency have demonstrated a reduction in the relative production of essential fatty
849 acids resulting in negative reproductive effects on primary consumers (Meyers et al., 2019). In this context, our IPL results
850 reveal modifications (among polar head groups, carbon numbers, and unsaturations) in response to divergent environmental
851 conditions. However, further investigation of the relative concentrations and turnover rates between TAGs and IPLs, in
852 addition to the production of essential fatty acids, are critical next steps in assessing the impacts of IPL remodeling on trophic
853 transfer processes.

854

855 While IPLs are not a major source of cellular N compared to proteins, the highly labile nature of these molecules after cell
856 death may be a potential source of rapidly recycled N via bacterial hydrolysis. On average, N-bearing IPLs such as PCs or
857 BLs, consist of ~2% N by molecular weight (estimated based on a typical 700g/mol betaine lipid). Based on their abundance,
858 they could contribute as much as 10.7 nmol/L of inorganic N in the highly N depleted surface waters of this experiment.
859 Inorganic N species are exceedingly low, and often below the limit of detection ($< \sim 0.1 \mu\text{mol/L}$, see methods for details),
860 particularly in the surface samples for most of the experiment after the OMZ water addition. Thus, it is possible that the rapid
861 degradation and recycling of N from IPLs could prove to be an additional supply of N under extremely limiting conditions.
862 Given the diel variability in TAG production via eukaryotic phytoplankton and the potential impacts on energy and carbon
863 fluxes (Becker et al., 2018), further analysis is needed to determine at what temporal scale IPLs may be recycled for TAG
864 synthesis. While Becker et al. (2018) did not find evidence of diacylglycerol transferase (DGAT) activity related to diel cycles,
865 additional investigations of other transferases or lipases relevant to the degradation of IPLs (e.g., PDAT or PGD) are critical.

866

867 IPLs may also be an important intermediate in the surface ocean sulfur cycle. Sulfur metabolites produced by phytoplankton
868 (Durham et al., 2019) play central roles in microbial food webs by functioning in metabolism, contributing to membrane
869 structure, supporting osmotic and redox balance, and acting as allelochemicals and signaling molecules (Moran and Durham,
870 2019). SQDGs are highly abundant IPLs, particularly in surface waters, and can constitute up to 60 nmol S/L, potentially
871 contributing to a significant proportion of the dissolved organic S in this region (ranging from $\sim 100\text{-}225 \text{ nmol/L}$; Lennartz et
872 al., 2019). The ability to catabolize SQDGs is widespread in heterotrophic bacteria and provides a highly ubiquitous source of
873 sulfur (and carbon) substrates in the synthesis of other essential sulfur metabolites (Speciale et al., 2016). As such, SQDGs are
874 considered major contributors to the global biosulfur cycle (Goddard-Borger and Williams, 2017) and their considerable
875 production in phytoplankton membranes may be augmented by changes in temperature, light availability (i.e., shading effects),
876 and pH (see discussion above).

877

878 Lipids are also sources of dissolved organic carbon (DOC) following hydrolysis by bacterial extracellular enzymes (Myklestad,
879 2000). Lipids have been observed as the most highly aged component of DOC and are considerably longer lived than lipids
880 found in suspended POC (Loh et al., 2004). However, much of the DOC pool remains uncharacterized (Nebbioso and Piccolo,
881 2013; Hansell and Carlson, 2014) and little is known regarding the specific processes forming refractory DOC fractions
882 (Hansell, 2013). Yet, preliminary estimates of the total production of relatively refractory DOC ($>100\text{-year}$ lifetime) suggest
883 potential significance to global biogeochemistry (Legendre et al., 2015). Furthermore, it is yet unclear as to how DOC cycling
884 may be affected by changing ocean conditions (Wagner et al., 2020). Understanding the degradation pathways involved with
885 abundant lipid pools and how they may contribute to the DOC pool in the surface ocean is of crucial importance to constraining
886 the fluxes of refractory organic carbon pools.

887

888 5 Conclusions

889 We investigated the potential for phytoplankton to evoke lipid remodeling in response to multiple environmental stressors
890 during a two-month mesocosm experiment in the Eastern Tropical South Pacific Ocean off the coast of Peru. Our study is
891 motivated by the need of understanding how the expected changes in oceanographic conditions due to climate forcing in this
892 area will impact the phytoplanktonic community driving primary productivity in the surface ocean, the chemistry of their cell
893 membranes, and thus the chemical composition of particulate organic matter. A key aspect of our efforts was to statistically
894 separate the relative roles of phytoplankton community composition and lipid remodeling in response to multiple
895 environmental stressors on the composition of the environmental algal lipidome over time. By using a combination of multiple
896 linear regressions, classification and regression trees, and random forest analyses, we report evidence of multiple
897 environmental variables potentially imparting controls on IPL head groups, many of which are known to have specific
898 functions in the chloroplast. The main takeaways of our study include:

- 899 ● IPLs are effective predictors of changes in the prevailing sources of phytoplankton biomass throughout the experiment.
- 900 ● The proportion of glycolipids (MGDG and SQDG) increases at higher temperatures, possibly to maintain thermal stability
901 of the photosynthetic apparatus in response to thermal stress.
- 902 ● The relationship between light levels and the distribution of MGDGs and PGs possibly invokes photoprotective and
903 antioxidant mechanisms provided by MGDGs, as well as the role of PGs in electron transport processes in photosystems
904 I and II.
- 905 ● Differences in the abundance of glycolipids between surface and subsurface waters appear to covary with oxygen
906 availability. We expect this difference to be driven by the degradation of MGDGs and DGDGs under anaerobiosis or
907 oxygen stress.
- 908 ● The reduction in N-bearing IPLs (i.e. BLs and PE) and the higher abundance of non-N-bearing IPLs (i.e., PG, SQDG and
909 MGDG) under more N-limited conditions suggests a possible IPL substitution mechanism to compensate for N limitation.
- 910 ● Whereas our study does not include the analysis of TAGs, our results are consistent with broader work suggesting that
911 IPLs may be used as a substrate for the generation of acyl chains in TAG production in response to environmental stressors
912 such as N limitation, variable pH or inorganic carbon availability, hypoxia, and varying light levels. However, such
913 mechanism in this mesocosm experiment remains to be tested in future work.
- 914 ● The cellular adaptations listed above likely contribute to the observed shifts in cellular content from structural or
915 extrachloroplastic membrane lipids (i.e., PCs, PEs, BLs, and certain PGs) under high growth conditions, to
916 thylakoid/plastid membrane lipids (i.e., MGDGs, DGDGs, SQDGs, and certain PGs) while exposed to environmental
917 stressors.

918 We hypothesize that these remodeling processes may involve major shifts in the elemental stoichiometry of the cell, and thus
919 alter the fluxes of C, N, and S to higher trophic levels, signaling potential impacts on the broader cycling of these biorelevant
920 elements under different scenarios of future environmental change. Therefore, we suggest that future studies addressing the

921 biogeochemical consequences of climate change in the Eastern Tropical South Pacific Ocean must include the role of lipid
922 remodeling in phytoplankton.

923

924 **Data availability**

925

926 The environmental study data are available at: <https://doi.org/10.1594/PANGAEA.923395> (Bach et al., 2020). Biomarkers
927 metadata that generates and supports the findings of this study and R code are available in: [https://github.com/Guachan/IPLS-](https://github.com/Guachan/IPLS-KOSMOS/tree/0.1.0)
928 [KOSMOS/tree/0.1.0](https://doi.org/10.5281/zenodo.10408453) (<https://doi.org/10.5281/zenodo.10408453>, Cantarero, 2023).

929

930 **Author contribution**

931

932 JS and SC designed the study. JS funded the study. JS and CV funded sample collection during the mesocosm experiment. UL
933 and LTB designed, funded, organized, and carried out the mesocosm experiment. PA, JS, LTB, and UR carried out sample
934 collection. SIC led laboratory and analytical work with the assistance of ND and under the supervision of JS. SEI carried out
935 data analysis. SIC, JET, BCS, and BR performed statistical analyzes. SIC wrote the manuscript with major editorial
936 contributions from EF, HA, and JS and with comments from all co-authors.

937

938

939 **Competing interests**

940

941 The authors declare that they have no conflict of interest. At least one of the (co-)authors is a member of the editorial board of
942 *Biogeosciences*.

943

944

945 **Acknowledgments**

946

947 We extend our gratitude to all participants in the KOSMOS Peru 2017 study for their invaluable assistance in mesocosm
948 sampling and maintenance. Our special thanks go to the dedicated staffs from GEOMAR-Kiel and IMARPE for their support
949 throughout the planning, preparation, and execution of this study. We are particularly grateful to A. Ludwig, M. Graco, D.
950 Gutierrez, A. Paul, S. Feiersinger, K. Schulz, J.P. Bednar, P. Fritsche, P. Stange, A. Schukat, and M. Krudewig. We also
951 express our appreciation to the captains and crews of BAP Morales, IMARPE VI, and BIC Humboldt for their support during
952 the deployment and recovery of the mesocosms. We extend special thanks to the Marina de Guerra del Perú, specifically the
953 submarine section of the navy in Callao, the Dirección General de Capitanías y Guardacostas, and the Club Náutico Del Centro
954 Naval. The KOSMOS Peru 2017 took place within the framework of the cooperation agreement between IMARPE and
955 GEOMAR through the German Federal Ministry of Education and Research (BMBF) project ASLAEEL 12-016 and the national
956 project Integrated Study of the Upwelling System off Peru developed by the Directorate of Oceanography and Climate Change
957 of IMARPE, PPR 137 CONCYTEC. We acknowledge all members of the Organic Geochemistry Laboratory in addition to K.
958 Rempfert, S. Kopf, T. Marchitto, N. Lovenduski at the University of Colorado Boulder, and M. Long at NCAR, for fruitful
959 discussions.

960

961 **Financial support**

962

963 This study was funded by the US National Science Foundation CAREER Award 2047057 "Microbial Lipidomics in Changing
964 Oceans" (MILCO) to J. Sepúlveda. S. Cantarero and J. Sepúlveda acknowledge additional support from the Department of
965 Geological Sciences and the Center for the Study of Origins at the University of Colorado Boulder. We thank the Millennium
966 Institute of Oceanography (IMO) ICN12_019 through the Agencia Nacional de Investigación y Desarrollo (ANID)—
967 Millennium Science Initiative Program—for providing funding for sample collection. The KOSMOS Peru 2017 was funded
968 by the Collaborative Research Centre SFB 754 Climate-Biogeochemistry Interactions in the Tropical Ocean, funded by the
969 German Research Foundation (DFG) to U. Riebesell. Additional funding was provided by the EU project AQUACOSM

970 through the European Union's Horizon 2020 research and innovation program under grant agreement no. 731065 and through
971 the Leibniz Award 2012, granted to Ulf Riebesell.

973 **References**

- 974 Abida, H., Dolch, L.J., Meï, C., Villanova, V., Conte, M., Block, M.A., Finazzi, G., Bastien, O., Tirichine, L., Bowler, C.,
975 Rébeillé, F., Petroustos, D., Jouhet, J., Maréchal, E.: Membrane glycerolipid remodeling triggered by nitrogen and
976 phosphorus starvation in *Phaeodactylum tricornutum*. *Plant Physiology*, 167, 118–136, ,
977 <https://doi.org/10.1104/pp.114.252395>, 2015. Abrahams, A., Schlegel, R. W., and Smit, A. J.: Variation and change of
978 upwelling dynamics detected in the world's eastern boundary upwelling systems, *Front. Mar. Sci.*, 8, 626411, doi:
979 10.3389/fmars.2021.626411, 2021.
- 980 Aristegui, J. and Harrison, W. G.: Decoupling of primary production and community respiration in the ocean: Implications for
981 regional carbon studies, *Aquat. Microb. Ecol.*, 29(2), 199–209, doi:10.3354/ame029199, 2002.
- 982 Arrigo, K. R.: Marine microorganisms and global nutrient cycles, *Nature*, 437(7057), 349–355, doi:10.1038/nature04159,
983 2005.
- 984 Azov, Y.: Effect of pH on inorganic carbon uptake in algal cultures, *Appl. Environ. Microbiol.*, 43(6), 1300–1306,
985 doi:10.1128/aem.43.6.1300-1306.1982, 1982.
- 986 Bach, L. T., Alvarez-Fernandez, S., Hornick, T., Stuhr, A. and Riebesell, U.: Simulated ocean acidification reveals winners
987 and losers in coastal phytoplankton, *PLoS One*, 12(11), 1–22, doi: 10.1371/journal.pone.0188198, 2017.
- 988 Bach, L. T., Paul, A. J., Boxhammer, T., von der Esch, E., Graco, M., Schulz, K. G., Achterberg, E., Aguayo, P., Aristegui, J.,
989 Ayón, P., Baños, I., Bernales, A., Boegeholz, A. S., Chavez, F., Chavez, G., Chen, S. M., Doering, K., Filella, A., Fischer,
990 M., Grasse, P., Haunost, M., Hennke, J., Hernández-Hernández, N., Hopwood, M., Igarza, M., Kalter, V., Kittu, L.,
991 Kohnert, P., Ledesma, J., Lieberum, C., Lischka, S., Löscher, C., Ludwig, A., Mendoza, U., Meyer, J., Meyer, J.,
992 Minutolo, F., Cortes, J. O., Piiparinen, J., Sforza, C., Spilling, K., Sanchez, S., Spisla, C., Sswat, M., Moreira, M. Z. and
993 Riebesell, U.: Factors controlling plankton community production, export flux, and particulate matter stoichiometry in
994 the coastal upwelling system off Peru, *Biogeosciences*, 17(19), 4831–4852, doi:10.5194/bg-17-4831-2020, 2020.
- 995 Bakun, A., Field, D. B., Redondo-Rodriguez, A. and Weeks, S. J.: Greenhouse gas, upwelling-favorable winds, and the future
996 of coastal ocean upwelling ecosystems, *Glob. Chang. Biol.*, 16(4), 1213–1228, doi:10.1111/j.1365-2486.2009.02094.x,
997 2010.
- 998 Barlow, R. G., Cummings, D. G. and Gibb, S. W.: Improved resolution of mono- and divinyl chlorophylls a and b and
999 zeaxanthin and lutein in phytoplankton extracts using reverse phase C-8 HPLC, *Mar. Ecol. Prog. Ser.*, 161, 303–307,
1000 <http://www.jstor.org/stable/24859034>, 1997.
- 1001 Becker, K.W., Collins, J.R., Durham, B.P., Groussman, R.D., White, A.E., Fredricks, H.F., Ossolinski, J.E., Repeta, D.J.,
1002 Carini, P., Armbrust, E.V. and Van Mooy, B.A., Daily changes in phytoplankton lipidomes reveal mechanisms of energy
1003 storage in the open ocean. *Nature communications* 9, 5179, <https://doi.org/10.1038/s41467-018-07346-z>, 2018.

1004 Behrenfeld, M. J., O'Malley, R. T., Siegel, D. A., McClain, C. R., Sarmiento, J. L., Feldman, G. C., Milligan, A. J., Falkowski,
1005 P. G., Letelier, R. M. and Boss, E. S.: Climate-driven trends in contemporary ocean productivity, *Nature*, 444(7120),
1006 752–755, doi:10.1038/nature05317, 2006.

1007 Benjamini, Y., and Yosef Hochberg, Y., Controlling the False Discovery Rate: A Practical and Powerful Approach to Multiple
1008 Testing, *Journal of the Royal Statistical Society: Series B (Methodological)*, 57, 289–300, doi:10.1111/j.2517-
1009 6161.1995.tb02031.x, 1995.

1010 Berry, J. and Bjorkman, O.: Photosynthetic Response and Adaptation to Temperature in Higher Plants, *Annu. Rev. Plant*
1011 *Physiol.*, 31(1), 491–543, doi:10.1146/annurev.pp.31.060180.002423, 1980.

1012 Brandsma, J.: The origin and fate of intact polar lipids in the marine environment, PhD thesis, Dept. of Marine Organic
1013 Biogeochemistry, Royal Netherlands Institute for Sea Research (NIOZ), pp. 224, ISBN: 978-90-6266-286-9, 2011.

1014 Bligh, E. G., and Dyer, W.J.: A rapid method of total lipid extraction and purification, *Canadian journal of biochemistry and*
1015 *physiology*, 37(8), 911-917, doi:10.1139/o59-099, 1959.

1016 Biau G., and Scornet E. A random forest guided tour. *Test*; 25(2): 197–227, <https://doi.org/10.1007/s11749-016-0481-7>, 2016.

1017 Boulesteix, A. L., Janitza, S., Kruppa, J., & König, I. R.: Overview of random forest methodology and practical guidance with
1018 emphasis on computational biology and bioinformatics. *Wiley Interdisciplinary Reviews: Data Mining and Knowledge*
1019 *Discovery*, 2(6), 493–507, <https://doi.org/10.1002/widm.1072>, 2012.

1020 Breiman, L., Friedman, J.H., Olshen, R.A., & Stone, C.J.: *Classification And Regression Trees (1st ed.)*, Chapman and
1021 Hall/CRC, <https://doi.org/10.1201/9781315139470>, 1984.

1022 Breiman, L.: Random Forests, *Mach. Learn.*, 45, 5–32, <https://doi.org/10.1023/A:1010933404324>, 2001.

1023 Browning, T. J., Rapp, I., Schlosser, C., Gledhill, M., Achterberg, E. P., Bracher, A. and Le Moigne, F. A. C.: Influence of
1024 Iron, Cobalt, and Vitamin B12 Supply on Phytoplankton Growth in the Tropical East Pacific During the 2015 El Niño,
1025 *Geophys. Res. Lett.*, 45(12), 6150–6159, doi:10.1029/2018GL077972, 2018.

1026 Bronk, D. A., See, J. H., Bradley, P., & Killberg, L.: DON as a source of bioavailable nitrogen for phytoplankton.
1027 *Biogeosciences*, 4(3), 283–296. <https://doi.org/10.5194/bg-4-283-2007>, 2007.

1028 Burian, A., Nielsen, J. M., Hansen, T., Bermudez, R. and Winder, M.: The potential of fatty acid isotopes to trace trophic
1029 transfer in aquatic food-webs, *Philos. Trans. R. Soc. B Biol. Sci.*, 375(1804), doi:10.1098/rstb.2019.0652, 2020.

1030 Cantarero, S., Henríquez-Castillo, C., Dildar, N., Vargas, C., von Dassow, P., Cornejo-D'Ottone, M. and Sepúlveda, J.: Size-
1031 fractionated contribution of microbial biomass to suspended organic matter in the Eastern Tropical South Pacific oxygen
1032 minimum zone, *Front. Mar. Sci.*, 7:540643. doi: 10.3389/fmars.2020.540643, 2020.

1033 Capone, D. G. and Hutchins, D. A.: Microbial biogeochemistry of coastal upwelling regimes in a changing ocean, *Nat. Geosci.*,
1034 6(9), 711–717, doi:10.1038/ngeo1916, 2013.

1035 Carter, B. R., Radich, J. A., Doyle, H. L. and Dickson, A. G.: An automated system for spectrophotometric seawater pH
1036 measurements, *Limnol. Oceanogr. Methods*, 11(JAN), 16–27, doi:10.4319/lom.2013.11.16, 2013.

- 1037 Chavez, F. P. and Messié, M.: A comparison of Eastern Boundary Upwelling Ecosystems, *Prog. Oceanogr.*, 83(1–4), 80–96,
1038 doi:10.1016/j.pocean.2009.07.032, 2009.
- 1039 Chen, S., Riebesell, U., Schulz, K. G., Esch, E. Von Der, Achterberg, E. P. and Bach, L. T.: Temporal dynamics of surface
1040 ocean carbonate chemistry in response to natural and simulated upwelling events during the 2017 coastal El Niño near
1041 Callao, Peru., *Biogeosciences*, 19,295-312, <https://doi.org/10.5194/bg-19-295-2022>, 2022.
- 1042 Chen, X., and H. Ishwaran.: Random forests for genomic data analysis. *Genomics* 99: 323–329,
1043 <https://doi.org/10.1016/j.ygeno.2012.04.003>, 2012. Coverly, S., Kérouel, R. and Aminot, A.: A re-examination of matrix
1044 effects in the segmented-flow analysis of nutrients in sea and estuarine water, *Anal. Chim. Acta*, 712, 94–100,
1045 doi:10.1016/j.aca.2011.11.008, 2012.
- 1046 Dahlgvist, A., Ståhl, U., Lenman, M., Banas, A., Lee, M., Sandager, L., Ronne, H. and Stymne, S.: Phospholipid:diacylglycerol
1047 acyltransferase: An enzyme that catalyzes the acyl-CoA-independent formation of triacylglycerol in yeast and plants,
1048 *Proc. Natl. Acad. Sci. U. S. A.*, 97(12), 6487–6492, doi:10.1073/pnas.120067297, 2000.
- 1049 Ding, H. and Sun, M. Y.: Biochemical degradation of algal fatty acids in oxic and anoxic sediment-seawater interface systems:
1050 Effects of structural association and relative roles of aerobic and anaerobic bacteria, *Mar. Chem.*, 93(1), 1–19,
1051 doi:10.1016/j.marchem.2004.04.004, 2005.
- 1052 DiTullio, G. R., Geesey, M. E., Mancher, J. M., Alm, M. B., Riseman, S. F. and Bruland, K. W.: Influence of iron on algal
1053 community composition and physiological status in the Peru upwelling system, *Limnol. Oceanogr.*, 50(6), 1887–1907,
1054 doi:10.4319/lo.2005.50.6.1887, 2005.
- 1055 Durham, B. P., Boysen, A. K., Carlson, L. T., Groussman, R. D., Heal, K. R., Cain, K. R., Morales, R. L., Coesel, S. N.,
1056 Morris, R. M., Ingalls, A. E. and Armbrust, E. V.: Sulfonate-based networks between eukaryotic phytoplankton and
1057 heterotrophic bacteria in the surface ocean, *Nat. Microbiol.*, 4(10), 1706–1715, doi:10.1038/s41564-019-0507-5, 2019.
- 1058 Dutkiewicz, S., Ward, B. A., Monteiro, F. and Follows, M. J.: Interconnection of nitrogen fixers and iron in the Pacific Ocean:
1059 Theory and numerical simulations, *Global Biogeochem. Cycles*, 26(1), 1–16, doi:10.1029/2011GB004039, 2012.
- 1060 Dutkiewicz, S., Morris, J. J., Follows, M. J., Scott, J., Levitan, O., Dyhrman, S. T. and Berman-Frank, I.: Impact of ocean
1061 acidification on the structure of future phytoplankton communities, *Nat. Clim. Chang.*, 5(11), 1002–1006,
1062 doi:10.1038/nclimate2722, 2015.
- 1063 Elsayed, K. N. M., Kolesnikova, T. A., Noke, A. and Klöck, G.: Imaging the accumulated intracellular microalgal lipids as a
1064 response to temperature stress, *3 Biotech*, 7(1), doi:10.1007/s13205-017-0677-x, 2017.
- 1065 Missing: Fabregas et al 2004 from 4.2.5 light availability
- 1066 Fakhry, E. M. and El Maghraby, D. M.: Lipid accumulation in response to nitrogen limitation and variation of temperature in
1067 *nannochloropsis salina*, *Bot. Stud.*, 56, 6, doi:10.1186/s40529-015-0085-7, 2015.
- 1068 Fan, J., Andre, C. and Xu, C.: A chloroplast pathway for the de novo biosynthesis of triacylglycerol in *Chlamydomonas*
1069 *reinhardtii*, *FEBS Lett.*, 585(12), 1985–1991, doi:10.1016/j.febslet.2011.05.018, 2011.

- 1070 Fuenzalida, R., Schneider, W., Garcés-Vargas, J., Bravo, L. and Lange, C.: Vertical and horizontal extension of the oxygen
1071 minimum zone in the eastern South Pacific Ocean, *Deep. Res. Part II Top. Stud. Oceanogr.*, 56(16), 992–1003,
1072 doi:10.1016/j.dsr2.2008.11.001, 2009.
- 1073 Gabruk, M., Mysliwa-Kurdziel, B., and Kruk, J.: MGDG, PG and SQDG regulate the activity of light-dependent
1074 protochlorophyllide oxidoreductase. *Biochem. J.* 474, 1307–1320. doi: 10.1042/BCJ20170047, 2017.
- 1075 Gardner, R. D., Cooksey, K. E., Mus, F., Macur, R., Moll, K., Eustance, E., Carlson, R. P., Gerlach, R., Fields, M. W. and
1076 Peyton, B. M.: Use of sodium bicarbonate to stimulate triacylglycerol accumulation in the chlorophyte *Scenedesmus* sp.
1077 and the diatom *Phaeodactylum tricornutum*, *J. Appl. Phycol.*, 24(5), 1311–1320, doi:10.1007/s10811-011-9782-0, 2012.
- 1078 Gardner, R., Peters, P., Peyton, B. and Cooksey, K. E.: Medium pH and nitrate concentration effects on accumulation of
1079 triacylglycerol in two members of the chlorophyta, *J. Appl. Phycol.*, 23(6), 1005–1016, doi:10.1007/s10811-010-9633-
1080 4, 2011.
- 1081 Gašparović, B., Godrijan, J., Frka, S., Tomažić, I., Penezić, A., Marić, D., Djakovac, T., Ivančić, I., Paliaga, P., Lyons, D.,
1082 Precali, R. and Tepić, N.: Adaptation of marine plankton to environmental stress by glycolipid accumulation, *Mar.*
1083 *Environ. Res.*, 92, 120–132, doi:10.1016/j.marenvres.2013.09.009, 2013.
- 1084 Geider, J. R. and Osborne, B. A.: Respiration and microalgal growth: a review of the quantitative relationship between dark
1085 respiration and growth, *New Phytol.*, 112(3), 327–341, doi:10.1111/j.1469-8137.1989.tb00321.x, 1989.
- 1086 Gilly, W. F., Beman, J. M., Litvin, S. Y. and Robison, B. H.: Oceanographic and Biological Effects of Shoaling of the Oxygen
1087 Minimum Zone, *Ann. Rev. Mar. Sci.*, 5(1), 393–420, doi:10.1146/annurev-marine-120710-100849, 2013.
- 1088 Goddard-Borger, and E.D., Williams, S.J., Sulfoquinovose in the biosphere: occurrence, metabolism and functions. *Biochem*
1089 *J* 1, 474 (5), 827–849, doi: <https://doi.org/10.1042/BCJ20160508>, 2017.
- 1090 Gombos, Z. and Murata, N.: Lipids and fatty acids of prochlorothrix hollandica, *Plant Cell Physiol.*, 32(1), 73–77,
1091 doi:10.1093/oxfordjournals.pcp.a078054, 1991.
- 1092
- 1093 Gonçalves, A. L., Pires, J. C., & Simões, M.: Lipid production of *Chlorella vulgaris* and *Pseudokirchneriella subcapitata*. *Int.*
1094 *J. Energy Environ. Eng.*, 4, 14, <https://doi.org/10.1186/2251-6832-4-14> 2013.
- 1095 Goss, R., Nerlich, J., Lepetit, B., Schaller, S., Vieler, A. and Wilhelm, C.: The lipid dependence of diadinoxanthin de-
1096 epoxidation presents new evidence for a macrodomain organization of the diatom thylakoid membrane, *J. Plant Physiol.*,
1097 166(17), 1839–1854, doi:10.1016/j.jplph.2009.05.017, 2009.
- 1098 Gu, X., Cao, L., Wu, X., Li, Y., Hu, Q. and Han, D.: A lipid bodies-associated galactosyl hydrolase is involved in
1099 triacylglycerol biosynthesis and galactolipid turnover in the unicellular green alga *Chlamydomonas reinhardtii*, *Plants*,
1100 10(4), doi:10.3390/plants10040675, 2021.
- 1101 Guckert, J. B., and Cooksey, K.E.: Triglyceride accumulation and fatty acid profile changes in *Chlorella* (Chlorophyta) during
1102 high Ph-induced cell cycle Inhibition, *Journal of Phycology*, 26, 72-79, <https://doi.org/10.1111/j.0022->
1103 3646.1990.00072.x, 1990.

- 1104 Guschina, I. A., and Harwood, J. L. Algal lipids and their metabolism. In: Borowitzka, M., Moheimani, N. (eds) *Algae for*
1105 *Biofuels and Energy*. Springer, Dordrecht, pp. 17-36. https://doi.org/10.1007/978-94-007-5479-2_2, 2013.
- 1106 Gutiérrez, D., Bouloubassi, I., Sifeddine, A., Purca, S., Goubanova, K., Graco, M., Field, D., Méjanelle, L., Velazco, F., Lorre,
1107 A., Salvattecchi, R., Quispe, D., Vargas, G., Dewitte, B. and Ortlieb, L.: Coastal cooling and increased productivity in the
1108 main upwelling zone off Peru since the mid-twentieth century, *Geophys. Res. Lett.*, 38(7), 1–6,
1109 doi:10.1029/2010GL046324, 2011.
- 1110 Hallegraeff, G.M. Ocean climate change, phytoplankton community responses, and harmful algal blooms: a formidable
1111 predictive challenge. *J. Phycol.* 46 (2), 220–235, <https://doi.org/10.1111/j.1529-8817.2010.00815.x>, 2010.
- 1112 Hansell, D. A.: Recalcitrant dissolved organic carbon fractions, *Ann. Rev. Mar. Sci.*, 5, 421–445, doi:10.1146/annurev-marine-
1113 120710-100757, 2013.
- 1114 Hansell, D. A., and Carlson, C.A., eds. *Biogeochemistry of marine dissolved organic matter*. Academic Press,
1115 <https://doi.org/10.1016/C2012-0-02714-7>, 2014.
- 1116 Harwood, J. L. and Jones, A. L.: Lipid Metabolism in Algae., *Advances in Botanical Research*, 16, 1-53,
1117 [https://doi.org/10.1016/S0065-2296\(08\)60238-4](https://doi.org/10.1016/S0065-2296(08)60238-4), 1989.
- 1118 Hastie, T., Tibshirani, R. and Friedman, J.: *Springer Series in Statistics, Elem. Stat. Learn.*, 27(2), 83–85, doi:10.1007/b94608,
1119 2009.
- 1120 Hauss, H., Franz, J., and Sommer, U.: Changes in N:P stoichiometry influence taxonomic composition and nutritional quality
1121 of phytoplankton in the Peruvian upwelling, *J. Sea Res.*, 73, 74–85, <https://doi.org/10.1016/j.seares.2012.06.010>, 2012.
- 1122 Hemschemeier, A., Casero, D., Liu, B., Benning, C., Pellegrini, M., Happe, T. and Merchant, S. S.: COPPER RESPONSE
1123 REGULATOR1-dependent and -independent responses of the *Chlamydomonas reinhardtii* transcriptome to dark anoxia,
1124 *Plant Cell*, 25(9), 3186–3211, doi:10.1105/tpc.113.115741, 2013.
- 1125 Henson, S. A., Cael, B. B., Allen, S. R. and Dutkiewicz, S.: Future phytoplankton diversity in a changing climate, *Nat.*
1126 *Commun.*, 12(1), 1–8, doi:10.1038/s41467-021-25699-w, 2021.
- 1127 Holm, H. C., Fredricks, H. F., Bent, S. M., Lowenstein, D. P., Ossolinski, J. E., Becker, K. W., Johnson, W. M., Schrage, K.,
1128 & Van Mooy, B. A. S. Global Ocean lipidomes show a universal relationship between temperature and lipid unsaturation.
1129 *Science*, 376, 1487– 1491. <https://doi.org/10.1126/science.abn7455>, 2022.
- 1130 Hu, Q., Sommerfeld, M., Jarvis, E., Ghirardi, M., Posewitz, M., Seibert, M. and Darzins, A.: Microalgal triacylglycerols as
1131 feedstocks for biofuel production: Perspectives and advances, *Plant J.*, 54(4), 621–639, doi:10.1111/j.1365-
1132 313X.2008.03492.x, 2008.
- 1133 Huertas E., I., Rouco, M., López-Rodas, V. and Costas, E.: Warming will affect phytoplankton differently: Evidence through
1134 a mechanistic approach, *Proc. R. Soc. B Biol. Sci.*, 278(1724), 3534–3543, doi:10.1098/rspb.2011.0160, 2011.
- 1135 Hutchins, D. A., Hare, C. E., Weaver, R. S., Zhang, Y., Firme, G. F., DiTullio, G. R., Alm, M. B., Riseman, S. F., Maucher,
1136 J. M., Geesey, M. E., Trick, C. G., Smith, G. J., Rue, E. L., Conn, J. and Bruland, K. W.: Phytoplankton iron limitation

1137 in the Humboldt Current and Peru Upwelling, *Limnol. Oceanogr.*, 47(4), 997–1011, doi:10.4319/lo.2002.47.4.0997,
1138 2002.

1139 Hutchins, D. A. and Fu, F.: Microorganisms and ocean global change, *Nat. Microbiol.*, 2(May),
1140 doi:10.1038/nmicrobiol.2017.58, 2017.

1141 Irwin, A. J., Finkel, Z. V., Müller-Karger, F. E. and Ghinaglia, L. T.: Phytoplankton adapt to changing ocean environments,
1142 *Proc. Natl. Acad. Sci. U. S. A.*, 112(18), 5762–5766, doi:10.1073/pnas.1414752112, 2015.

1143 Jiang, L., Luo, S., Fan, X., Yang, Z. and Guo, R.: Biomass and lipid production of marine microalgae using municipal
1144 wastewater and high concentration of CO₂, *Appl. Energy*, 88(10), 3336–3341, doi:10.1016/j.apenergy.2011.03.043,
1145 2011.

1146 Jiang, L. Q., Carter, B. R., Feely, R. A., Lauvset, S. K. and Olsen, A.: Surface ocean pH and buffer capacity: past, present and
1147 future, *Sci. Rep.*, 9(1), 1–11, doi:10.1038/s41598-019-55039-4, 2019.

1148 Jin, P., Liang, Z., Lu, H., Pan, J., Li, P., Huang, Q., Guo Y., Zhong, J., Li, F., Wan, J., Overmans, S., and Xia, J.: Lipid
1149 remodeling reveals the adaptations of a marine diatom to ocean acidification. *Frontiers in Microbiology*, 12, 748445,
1150 doi: 10.3389/fmicb.2021.748445, 2021.

1151 Jónasdóttir, S. H.: Fatty acid profiles and production in marine phytoplankton, *Mar. Drugs*, 17(3), doi:10.3390/md17030151,
1152 2019.

1153 Kato, C., Masui, N., and Horikoshi, K.: Properties of obligately barophilic bacteria isolated from a sample of deep-sea sediment
1154 from the Izu-Bonin trench, *J. Mar. Biotechnol.*, 4, 96-99, <https://cir.nii.ac.jp/crid/1573105973909199488>, 1996.

1155 Keeling, R. F., Körtzinger, A. and Gruber, N.: Ocean deoxygenation in a warming world, *Ann. Rev. Mar. Sci.*, 2(1), 199–229,
1156 doi:10.1146/annurev.marine.010908.163855, 2010.

1157 Kérouel, R. and Aminot, A.: Fluorometric determination of ammonia in sea and estuarine waters by direct segmented flow
1158 analysis, *Mar. Chem.*, 57(3–4), 265–275, doi:10.1016/S0304-4203(97)00040-6, 1997.

1159 Khoeyi, Z. A., Seyfabadi, J. and Ramezanpour, Z.: Effect of light intensity and photoperiod on biomass and fatty acid
1160 composition of the microalgae, *Chlorella vulgaris*, *Aquac. Int.*, 20(1), 41–49, doi:10.1007/s10499-011-9440-1, 2012.

1161 Khotimchenko, S. V. and Yakovleva, I. M.: Lipid composition of the red alga *Tichocarpus crinitus* exposed to different levels
1162 of photon irradiance, *Phytochemistry*, 66(1), 73–79, doi:10.1016/j.phytochem.2004.10.024, 2005.

1163 Khotimchenko, S. V. and Yakovleva, I. M.: Effect of solar irradiance on lipids of the green alga *Ulva fenestrata* Postels et
1164 Ruprecht, *Bot. Mar.*, 47(5), 395–401, doi:10.1515/BOT.2004.050, 2004.

1165 Kobayashi, K., Endo, K. and Wada, H.: Specific distribution of phosphatidylglycerol to photosystem complexes in the
1166 thylakoid membrane, *Front. Plant Sci.*, 8(November), 1–7, doi:10.3389/fpls.2017.01991, 2017.

1167 Kong, F., Romero, I. T., Warakanont, J. and Li-Beisson, Y.: Lipid catabolism in microalgae, *New Phytol.*, 218(4), 1340–1348,
1168 doi:10.1111/nph.15047, 2018.

1169 Kudela, R. M., Seeyave, S., and Cochlan, W. P.: The role of nutrients in regulation and promotion of harmful algal blooms in
1170 upwelling systems, *Prog. Oceanogr.*, 85, 122–135, <https://doi.org/10.1016/j.pocean.2010.02.008>, 2010.

1171 Kumari, P., Bijo, A. J., Mantri, V. A., Reddy, C. R. K. and Jha, B.: Fatty acid profiling of tropical marine macroalgae: An
1172 analysis from chemotaxonomic and nutritional perspectives, *Phytochemistry*, 86, 44–56,
1173 doi:10.1016/j.phytochem.2012.10.015, 2013.

1174 Lam, P., Kuypers, M. M. M., Lavik, G., Jensen, M. M., Vossenberg, J. Van De, Schmid, M., Woebken, D., Amann, R., Jetten,
1175 M. S. M. and Kuypers, M. M. M.: Revising the nitrogen cycle in the Peruvian oxygen minimum zone Phyllis, *Proc. Natl.*
1176 *Acad. Sci.*, 106(12), 2192–2205, doi:10.1038/nature0415, 2009.

1177 Legendre, L., Rivkin, R. B., Weinbauer, M. G., Guidi, L. and Uitz, J.: The microbial carbon pump concept: Potential
1178 biogeochemical significance in the globally changing ocean, *Prog. Oceanogr.*, 134, 432–450,
1179 doi:10.1016/j.pocean.2015.01.008, 2015.

1180 Lennartz, S., von Hobe, M., Booge, D., Bittig, H., Fischer, T., Gonçalves-Araujo, R., Ksionzek, K., Koch, B., Bracher, A.,
1181 Röttgers, R., Quack, B. and Marandino, C.: The influence of dissolved organic matter on the marine production of
1182 carbonyl sulfide (OCS) and carbon disulfide (CS₂) in the Eastern Tropical South Pacific, *Ocean Sci. Discuss.*, (March),
1183 1–32, doi:10.5194/os-2019-1, 2019.

1184 Li, X., Benning, C., & Kuo, M. H.: Rapid triacylglycerol turnover in *Chlamydomonas reinhardtii* requires a lipase with broad
1185 substrate specificity. *Eukaryotic Cell*, 11(12), 1451-1462, doi: 10.1128/EC.00268-12, 2012.

1186 Li-Beisson, Y., Thelen, J. J., Fedosejevs, E. and Harwood, J. L.: The lipid biochemistry of eukaryotic algae, *Prog. Lipid Res.*,
1187 74, 31–68, doi:10.1016/j.plipres.2019.01.003, 2019.

1188 Lipp, J. S., Morono, Y., Inagaki, F., and Hinrichs, K.-U.: Significant contribution of Archaea to extant biomass in marine
1189 subsurface sediments, *Nature*, 454, 991–994, <https://doi.org/10.1038/nature07174>, 2008.

1190 Liu, J., Yuan, C., Hu, G. and Li, F.: Effects of light intensity on the growth and lipid accumulation of microalga *Scenedesmus*
1191 *sp.* 11-1 under nitrogen limitation, *Appl. Biochem. Biotechnol.*, 166(8), 2127–2137, doi:10.1007/s12010-012-9639-2,
1192 2012.

1193 Liu, B.: Biochemical Characterization of Triacylglycerol Metabolism in Microalgae, PhD thesis, Biochemistry and Molecular
1194 Biology, Michigan State University, USA. pp. 165, ISBN: 97813037151741303715171, 2014.

1195 Loh, A. N., Bauer, J. E. and Druffel, E. R. M.: Variable ageing and storage of dissolved organic components in the open ocean,
1196 *Nature*, 430(7002), 877–881, doi:10.1038/nature02780, 2004.

1197 Luan, J., Zhang, C., Xu, B., Xue, Y., Ren, Y.: The predictive performances of random forest models with limited sample size
1198 and different species traits. *Fish. Res.* 227: 105534, <https://doi.org/10.1016/j.fishres.2020.105534>, 2020.

1199 Lyon, B. R. and
1200 Mock, T.: Polar microalgae: New approaches towards understanding adaptations to an extreme and changing
environment, *Biology (Basel)*, 3(1), 56–80, doi:10.3390/biology3010056, 2014.

1201 Mackey, M. D., Mackey, D. J., Higgins, H. W. and Wright, S. W.: CHEMTAX - A program for estimating class abundances
1202 from chemical markers: Application to HPLC measurements of phytoplankton, *Mar. Ecol. Prog. Ser.*, 144(1–3), 265–
1203 283, doi:10.3354/meps144265, 1996.

1204 Masuda, S., Kobayashi, M., Icochea Salas, L.A. and Rosales Quintana, G.M.: Possible link between temperatures in the
1205 seashore and open ocean waters of Peru identified by using new seashore water data. *Progr. Earth Planet. Sci.*, 10, 38,
1206 <https://doi.org/10.1186/s40645-023-00571-1>, 2023.

1207 Meador, T. B., Goldenstein, N. I., Gogou, A., Herut, B., Psarra, S., Tsagaraki, T. M. and Hinrichs, K. U.: Planktonic lipidome
1208 responses to Aeolian dust input in low-biomass oligotrophic marine mesocosms, *Front. Mar. Sci.*, 4(APR), 1–20,
1209 doi:10.3389/fmars.2017.00113, 2017.

1210 Messié, M., Ledesma, J., Kolber, D. D., Michisaki, R. P., Foley, D. G., & Chavez, F. P.: Potential new production estimates
1211 in four eastern boundary upwelling ecosystems. *Progress in Oceanography*, 83(1-4), 151-158, doi:
1212 <https://doi.org/10.1016/j.pocean.2009.07.018>, 2009.

1213 Messié, M. and Chavez, F. P.: Seasonal regulation of primary production in eastern boundary upwelling systems, *Prog.*
1214 *Oceanogr.*, 134, 1–18, doi:10.1016/j.pocean.2014.10.011, 2015.

1215 Meyer, J., Löscher, C. R., Lavik, G. and Riebesell, U.: Mechanisms of P* reduction in the eastern tropical South Pacific, *Front.*
1216 *Mar. Sci.*, 4(JAN), 1–12, doi:10.3389/fmars.2017.00001, 2017.

1217 Meyers, M. T., Cochlan, W. P., Carpenter, E. J. and Kimmerer, W. J.: Effect of ocean acidification on the nutritional quality
1218 of marine phytoplankton for copepod reproduction, *PLoS One*, 14(5), 1–22, doi:10.1371/journal.pone.0217047, 2019.

1219 Mimouni, V., Couzinet-Mossion, A., Ulmann, L., & Wielgosz-Collin, G.. Lipids from microalgae. In: Levine, I. A., Fleurence,,
1220 J. (Eds) *Microalgae in health and disease prevention*, pp. 109-131, Academic Press, doi: 10.1016/B978-0-12-811405-
1221 6.00005-0, 2018.

1222 Min, M.A., Needham, D.M., Sudek, S., Truelove, N.K., Pitz, K.J., Chavez, G.M., Poirier, C., Gardeler, B., von der Esch, E.,
1223 Ludwig, A., Riebesell, U., Worden, A.Z., Chavez, F.P., 2023. Ecological divergence of a mesocosm in an eastern
1224 boundary upwelling system assessed with multi-marker environmental DNA metabarcoding. *Biogeosciences* 20, 1277–
1225 1298. <https://doi.org/10.5194/bg-20-1277-2023>, 2023.

1226 Moazami-Goudarzi, M. and Colman, B.: Changes in carbon uptake mechanisms in two green marine algae by reduced seawater
1227 pH, *J. Exp. Mar. Bio. Ecol.*, 413, 94–99, doi:10.1016/j.jembe.2011.11.017, 2012.

1228 Mock, T. and Gradinger, R.: Changes in photosynthetic carbon allocation in algal assemblages of Arctic sea ice with
1229 decreasing nutrient concentrations and irradiance, *Mar. Ecol. Prog. Ser.*, 202, 1–11, doi:10.3354/meps202001, 2000.

1230 Morales, M., Aflalo, C. and Bernard, O.: Microalgal lipids: A review of lipids potential and quantification for 95 phytoplankton
1231 species, *Biomass and Bioenergy*, 150(April), 106108, doi:10.1016/j.biombioe.2021.106108, 2021.

1232 Morán, X. A. G., López-Urrutia, Á., Calvo-Díaz, A. and LI, W. K. W.: Increasing importance of small phytoplankton in a
1233 warmer ocean, *Glob. Chang. Biol.*, 16(3), 1137–1144, doi:10.1111/j.1365-2486.2009.01960.x, 2010.

1234 Moran, M. A. and Durham, B. P.: Sulfur metabolites in the pelagic ocean, *Nat. Rev. Microbiol.*, 17(11), 665–678,
1235 doi:10.1038/s41579-019-0250-1, 2019.

1236 Morris, A. W. and Riley, J. P.: The determination of nitrate in sea water, *Anal. Chim. Acta*, 29(C), 272–279,
1237 doi:10.1016/S0003-2670(00)88614-6, 1963.

- 1238 Mullin, J. B. and Riley, J. P.: The colorimetric determination of silicate with special reference to sea and natural waters, *Anal.*
1239 *Chim. Acta*, 12(C), 162–176, doi:10.1016/S0003-2670(00)87825-3, 1955.
- 1240 Murphy, J. and Riley, J. P.: A modified single solution method for the determination of phosphate in natural waters, *Anal.*
1241 *Chim. Acta*, 27(C), 31–36, doi:10.1016/S0003-2670(00)88444-5, 1962.
- 1242 Myklestad, S. M.: Dissolved Organic Carbon from Phytoplankton, In Wangersky, P. J., (Eds) *Marine Chemistry. The*
1243 *Handbook of Environmental Chemistry*, Springer, Berlin, Heidelberg, 111–148, doi:10.1007/10683826_5, 2000.
- 1244 Nakajima, Y., Umena, Y., Nagao, R., Endo, K., Kobayashi, K., Akita, F., Suga, M., Wada, H., Noguchi, T., and Shen, J. R.,
1245 Thylakoid membrane lipid sulfoquinovosyl-diacylglycerol (SQDG) is required for full functioning photosystem II in
1246 *Thermosynechococcus elongatus*, *J. Biol. Chem.*, 293, 14786-14797, <https://doi.org/10.1074/jbc.RA118.004304d>,
1247 2018.
- 1248 Naqvi, S. W. A., Bange, H., Farias, L., Monteiro, P., Scranton, M., & Zhang, J.: Marine hypoxia/anoxia as a source of CH₄
1249 and N₂O. *Biogeosciences*, 7, <https://doi.org/10.5194/bg-7-2159>, 2010. Nebbioso, A. and Piccolo, A.: Molecular
1250 characterization of dissolved organic matter (DOM): A critical review, *Anal. Bioanal. Chem.*, 405(1), 109–124,
1251 doi:10.1007/s00216-012-6363-2, 2013.
- 1252 Neidleman, S. L.: Effects of temperature on lipid unsaturation, *Biotechnol. Genet. Eng. Rev.*, 5(1), 245–268,
1253 doi:10.1080/02648725.1987.10647839, 1987.
- 1254 Orcutt, D. M. and Patterson, G. W.: Effect of light intensity upon lipid composition of *Nitzschia closterium* (*Cylindrotheca*
1255 *fusiformis*), *Lipids*, 9(12), 1000–1003, doi:10.1007/BF02533825, 1974.
- 1256 Oyarzún, D. and Brierley, C. M.: The future of coastal upwelling in the Humboldt current from model projections, *Clim.*
1257 *Dynam.*, 52, 599–615, <https://doi.org/10.1007/s00382-018-4158-7>, 2019.
- 1258 Pal, D., Khozin-Goldberg, I., Cohen, Z. and Boussiba, S.: The effect of light, salinity, and nitrogen availability on lipid
1259 production by *Nannochloropsis* sp., *Appl. Microbiol. Biotechnol.*, 90(4), 1429–1441, doi:10.1007/s00253-011-3170-1,
1260 2011.
- 1261 Paul, A. J., Bach, L. T., Schulz, K. G., Boxhammer, T., Czerny, J., Achterberg, E. P., Hellemann, D., Trense, Y., Nausch, M.,
1262 Sswat, M. and Riebesell, U.: Effect of elevated CO₂ on organic matter pools and fluxes in a summer Baltic Sea plankton
1263 community, *Biogeosciences*, 12(20), 6181–6203, doi:10.5194/bg-12-6181-2015, 2015.
- 1264 Peng, X., Liu, S., Zhang, W., Zhao, Y., Chen, L., Wang, H. and Liu, T.: Triacylglycerol accumulation of *Phaeodactylum*
1265 *tricornutum* with different supply of inorganic carbon, *J. Appl. Phycol.*, 26(1), 131–139, doi:10.1007/s10811-013-0075-
1266 7, 2014.
- 1267 Pitcher, G. C., Aguirre-Velarde, A., Breitburg, D., Cardich, J., Carstensen, J., Conley, D. J., Dewitte, B., Engel, A.,
1268 EspinozaMorriberón, D., Flores, G., Garçon, V., Graco, M., Grégoire, M., Gutiérrez, D., Hernandez-Ayon, J. M., Huang,
1269 H.-H. M., Isensee, K., Jacinto, M. E., Levin, L., Lorenzo, A., Machu, E., Merma, L., Montes, I., Swa, N., Paulmier, A.,
1270 Roman, M., Rose, K., Hood, R., Rabalais, N. N., Salvanes, A. G. V., Salvatelli, R., Sánchez, S., Sifeddine, A., Tall, A.

1271 W., Plas, A. K. v. d., Yasuhara, M., Zhang, J., and Zhu, Z. Y.: System controls of coastal and open ocean oxygen
1272 depletion, *Prog. Oceanogr.*, 197, 102613, <https://doi.org/10.1016/j.pocean.2021.102613>, 2021.

1273 Poerschmann, J., Spijkerman, E. and Langer, U.: Fatty acid patterns in *Chlamydomonas* sp. as a marker for nutritional regimes
1274 and temperature under extremely acidic conditions, *Microb. Ecol.*, 48(1), 78–89, doi:10.1007/s00248-003-0144-6, 2004.

1275 Pependorf, K.J., Lomas, M.W. and Van Mooy, B.A.: Microbial sources of intact polar diacylglycerolipids in the Western
1276 North Atlantic Ocean. *Organic geochemistry*, 42(7), pp.803-811, <https://doi.org/10.1016/j.orggeochem.2011.05.003>,
1277 2011.

1278 Popko, J., Herrfurth, C., Feussner, K., Ischebeck, T., Iven, T., Haslam, R., Hamilton, M., Sayanova, O., Napier, J., Khozin-
1279 Goldberg, I. and Feussner, I.: Metabolome analysis reveals betaine lipids as major source for triglyceride formation, and
1280 the accumulation of sedoheptulose during nitrogen-starvation of *Phaeodactylum tricornutum*, *PLoS One*, 11(10), 1–23,
1281 doi:10.1371/journal.pone.0164673, 2016.

1282 Raven, J. A., and Beardall, J.: Carbohydrate metabolism and respiration in algae, In Larkum, A. W. D., Douglas, S. S., Raven,
1283 J. A. (Eds) *Photosynthesis in algae*, 14, pp. 205-224, Springer, Dordrecht, [https://doi.org/10/1007/978-94-007-1038-
1284 2_10](https://doi.org/10/1007/978-94-007-1038-2_10), 2003.

1285 Riebesell, U., Czerny, J., Von Bröckel, K., Boxhammer, T., Büdenbender, J., Deckelnick, M., Fischer, M., Hoffmann, D.,
1286 Krug, S. A., Lentz, U., Ludwig, A., Mucbe, R. and Schulz, K. G.: Technical Note: A mobile sea-going mesocosm system
1287 - New opportunities for ocean change research, *Biogeosciences*, 10(3), 1835–1847, doi:10.5194/bg-10-1835-2013, 2013.

1288 Roessler, P. G. Environmental control of glycerolipid metabolism in microalgae: commercial implications and future research
1289 directions, *Journal of Phycology*, 26.3, 393-399, <https://doi.org/10/1111/j.0022-3646.1990.00383.x>, 1990.

1290 Russell, N. J., and Nichols, D. S.: Polyunsaturated fatty acids in marine bacteria—a dogma rewritten, *Microbiology*, 145.4,
1291 767-779, doi:10.1099/13500872-145-4-767, 1999.

1292 Rütters, H., Sass, H., Cypionka, H., and Rullkötter, J.: Monoalkylether phospholipids in the sulfate-reducing bacteria
1293 *Desulfosarcina variabilis* and *Desulforhabdus amnigenus*, *Arch. Microbiol.*, 176, 435–442, doi:
1294 10.1007/s002030100343, 2001.

1295 Sakamoto, T. and Murata, N.: Regulation of the desaturation of fatty acids and its role in tolerance to cold and salt stress, *Curr.*
1296 *Opin. Microbiol.*, 5(2), 206–210, doi:10.1016/S1369-5274(02)00306-5, 2002.

1297 Sakurai, I., Hagio, M., Gombos, Z., Tyystjärvi, T., Paakkarinen, V., Aro, E. M. and Wada, H.: Requirement of
1298 Phosphatidylglycerol for Maintenance of Photosynthetic Machinery, *Plant Physiol.*, 133(3), 1376–1384,
1299 doi:10.1104/pp.103.026955, 2003.

1300 Sato, N. and Murata, N.: Temperature shift-induced responses in lipids in the blue-green alga, *Anabaena variabilis*, *Biochim.*
1301 *Biophys. Acta - Lipids Lipid Metab.*, 619(2), 353–366, doi:10.1016/0005-2760(80)90083-1, 1980.

1302 Sato, N., Aoki, M., Maru, Y., Sonoike, K., Minoda, A. and Tsuzuki, M.: Involvement of sulfoquinovosyl diacylglycerol in the
1303 structural integrity and heat-tolerance of photosystem II, *Planta*, 217(2), 245–251, doi:10.1007/s00425-003-0992-9,
1304 2003.

- 1305 Sayanova, O., Mimouni, V., Ulmann, L., Morant-Manceau, A., Pasquet, V., Schoefs, B. and Napier, J. A.: Modulation of lipid
1306 biosynthesis by stress in diatoms, *Philos. Trans. R. Soc. B Biol. Sci.*, 372(1728), doi:10.1098/rstb.2016.0407, 2017.
- 1307 Schubotz, F., Wakeham, S. G., Lipp, J. S., Fredricks, H. F. and Hinrichs, K. U.: Detection of microbial biomass by intact polar
1308 membrane lipid analysis in the water column and surface sediments of the Black Sea, *Environ. Microbiol.*, 11(10), 2720–
1309 2734, doi:10.1111/j.1462-2920.2009.01999.x, 2009.
- 1310 Schubotz, F., Xie, S., Lipp, J. S., Hinrichs, K. and Wakeham, S. G.: Intact polar lipids in the water column of the eastern
1311 tropical North Pacific: abundance and structural variety of non-phosphorus lipids, *Biogeosciences*, 15, 6481-6501,
1312 <https://doi.org/10.5194/bg-15-6481-2018>, 2018.
- 1313 Sinensky, M.: Homeoviscous adaptation: a homeostatic process that regulates the viscosity of membrane lipids in *Escherichia*
1314 *coli*, *Proc. Natl. Acad. Sci. U. S. A.*, 71(2), 522–525, doi:10.1073/pnas.71.2.522, 1974.
- 1315 Singh, Y. and Kumar, H. D.: Lipid and hydrocarbon production by *Botryococcus* spp. under nitrogen limitation and
1316 anaerobiosis, *World J. Microbiol. Biotechnol.*, 8(2), 121–124, doi:10.1007/BF01195829, 1992.
- 1317 Smalley, G. W., Coats, D. W., and Stoecker, D. K.: Feeding in the mixotrophic dinoflagellate *Ceratium furca* is influenced by
1318 intracellular nutrient concentrations, *Mar. Ecol. Prog. Ser.*, 262, 137-151, doi:10.3354/meps262137, 2003.
- 1319 Speciale, G., Jin, Y., Davies, G. J., Williams, S. J. and Goddard-Borger, E. D.: YihQ is a sulfoquinovosidase that cleaves
1320 sulfoquinovosyl diacylglyceride sulfolipids, *Nat. Chem. Biol.*, 12(4), 215–217, doi:10.1038/nchembio.2023, 2016.
- 1321 Stramma, L., Johnson, G. C., Sprintall, J. and Mohrholz, V.: Expanding oxygen-minimum zones in the tropical oceans, *Science*
1322 , 320, 655–658, doi:10.1126/science.1153847, 2008.
- 1323 Stramma, L., Schmidtko, S., Levin, L. A. and Johnson, G. C.: Ocean oxygen minima expansions and their biological impacts,
1324 *Deep. Res. Part I Oceanogr. Res. Pap.*, 57(4), 587–595, doi:10.1016/j.dsr.2010.01.005, 2010.
- 1325 Sturt, H. F., Summons, R. E., Smith, K., Elvert, M. and Hinrichs, K. U.: Intact polar membrane lipids in prokaryotes and
1326 sediments deciphered by high-performance liquid chromatography/electrospray ionization multistage mass spectrometry
1327 - New biomarkers for biogeochemistry and microbial ecology, *Rapid Commun. Mass Spectrom.*, 18(6), 617–628,
1328 doi:10.1002/rem.1378, 2004.
- 1329 Sukenik, A., Zmora, O. and Carmeli, Y.: Biochemical quality of marine unicellular algae with special emphasis on lipid
1330 composition. II. *Nannochloropsis* sp., *Aquaculture*, 117(3–4), 313–326, doi:10.1016/0044-8486(93)90328-V, 1993.
- 1331 Suzumura, M.: Phospholipids in marine environments: a review, *Talanta*, 66, 422–434, doi: 10.1016/j.talanta.2004.12.008,
1332 2005.
- 1333 Tatsuzawa, H. and Takizawa, E.: Fatty Acid and Lipid Composition of the Acidophilic green alga *Chlamydomonas* Sp., *Journal*
1334 *of Phycology*, 32(4), 598–601, <https://doi.org/10.1111/j.0022-3646.1996.00598.x>, 1996.
- 1335 Taucher, J., Bach, L. T., Boxhammer, T., Nauendorf, A., Achterberg, E. P., Algueró-Muñiz, M., Arístegui, J., Czerny, J.,
1336 Esposito, M., Guan, W., Haunost, M., Horn, H. G., Ludwig, A., Meyer, J., Spisla, C., Sswat, M., Stange, P., Riebesell,
1337 U., Aberle-Malzahn, N., Archer, S., Boersma, M., Broda, N., Büdenbender, J., Clemmesen, C., Deckelnick, M., Dittmar,
1338 T., Dolores-Gelado, M., Dörner, I., Fernández-Urruzola, I., Fiedler, M., Fischer, M., Fritsche, P., Gomez, M., Grossart,

1339 H. P., Hattich, G., Hernández-Brito, J., Hernández-Hernández, N., Hernández-León, S., Hornick, T., Kolzenburg, R.,
1340 Krebs, L., Kreuzburg, M., Lange, J. A. F., Lischka, S., Linsenbarth, S., Löscher, C., Martínez, I., Montoto, T., Nachtigall,
1341 K., Osma-Prado, N., Packard, T., Pansch, C., Posman, K., Ramírez-Bordón, B., Romero-Kutzner, V., Rummel, C., Salta,
1342 M., Martínez-Sánchez, I., Schröder, H., Sett, S., Singh, A., Suffrian, K., Tames-Espinosa, M., Voss, M., Walter, E.,
1343 Wannicke, N., Xu, J. and Zark, M.: Influence of ocean acidification and deep water upwelling on oligotrophic plankton
1344 communities in the subtropical North Atlantic: Insights from an in situ mesocosm study, *Front. Mar. Sci.*, 4(APR),
1345 doi:10.3389/fmars.2017.00085, 2017.

1346 Thamdrup, B., Dalsgaard, T. and Revsbech, N. P.: Widespread functional anoxia in the oxygen minimum zone of the Eastern
1347 South Pacific, *Deep. Res. Part I Oceanogr. Res. Pap.*, 65, 36–45, doi:10.1016/j.dsr.2012.03.001, 2012.

1348 Tréguer, P., Bowler, C., Moriceau, B., Dutkiewicz, S., Gehlen, M., Aumont, O., Bittner, L., Dugdale, R., Finkel, Z., Iudicone,
1349 D., Jahn, O., Guidi, L., Lasbleiz, M., Leblanc, K., Levy, M., and Pondaven, P.: Influence of diatom diversity on the
1350 ocean biological carbon pump. *Nature Geosci.*, 11, 27–37, doi: <https://doi.org/10.1038/s41561-017-0028-x>, 2018.

1351 Tretkoff, E. Research Spotlight: Coastal cooling and marine productivity increasing off Peru. *Eos Transact. Am. Geophys.*
1352 *Union* 92, 184–184. doi: 10.1029/2011eo210009, 2011

1353 Twining, C. W., Taipale, S. J., Ruess, L., Bec, A., Martin-Creuzburg, D. and Kainz, M. J.: Stable isotopes of fatty acids:
1354 Current and future perspectives for advancing trophic ecology, *Philos. Trans. R. Soc. B Biol. Sci.*, 375(1804),
1355 doi:10.1098/rstb.2019.0641, 2020.

1356

1357 Tyrallis, H., Papacharalampous, G., & Langousis, A. A brief review of random forests for water scientists and practitioners and
1358 their recent history in water resources. *Water*, 11(5), 910, <https://doi.org/10.3390/w11050910>, 2019.

1359 Ulloa, O. and Pantoja, S.: The oxygen minimum zone of the eastern South Pacific, *Deep. Res. Part II Top. Stud. Oceanogr.*,
1360 56(16), 987–991, doi:10.1016/j.dsr2.2008.12.004, 2009.

1361 Van Mooy, B. A. S. and Fredricks, H. F.: Bacterial and eukaryotic intact polar lipids in the eastern subtropical South Pacific:
1362 Water-column distribution, planktonic sources, and fatty acid composition, *Geochim. Cosmochim. Acta*, 74(22), 6499–
1363 6516, doi:10.1016/j.gca.2010.08.026, 2010.

1364 Van Mooy, B. A. S., Fredricks, H. F., Pedler, B. E., Dyhrman, S. T., Karl, D. M., Koblížek, M., Lomas, M. W., Mincer, T. J.,
1365 Moore, L. R., Moutin, T., Rappé, M. S. and Webb, E. A.: Phytoplankton in the ocean use non-phosphorus lipids in
1366 response to phosphorus scarcity, *Nature*, 458(7234), 69–72, doi:10.1038/nature07659, 2009.

1367 Van Mooy, B. A., Rocap, G., Fredricks, H. F., Evans, C. T., and Devol, A. H.: Sulfolipids dramatically decrease phosphorus
1368 demand by picocyanobacteria in oligotrophic marine environments, *P. Natl. Acad. Sci. USA*, 103(23), 8607–8612,
1369 <https://doi.org/10.1073/pnas.0600540103>, 2006.

1370 Vargas, C. A., Cantarero, S. I., Sepúlveda, J. A., Galán, A., De Pol Holz, R., Walker, B., Schneider, W., Fariás, L., Cornejo
1371 D’Ottone, M., Walker, J., Xu, X., and Salisbury, J.: A source of isotopically light organic carbon in a low-pH anoxic
1372 marine zone. *Nature Communications*, 12, 1604. <https://doi.org/10.1038/s41467-021-21871-4>, 2021. Volkman, J. K.,

- 1373 Jeffrey, S. W., Nichols, P. D., Rogers, G. I. and Garland, C. D.: Fatty acid and lipid composition of 10 species of
1374 microalgae used in mariculture, *J. Exp. Mar. Bio. Ecol.*, 128(3), 219–240, doi:10.1016/0022-0981(89)90029-4, 1989.
- 1375 Volkman, J. K., Barrett, S. M., Blackburn, S. I., Mansour, M. P., Sikes, E. L. and Gelin, F.: Microalgal biomarkers: A review
1376 of recent research developments, *Org. Geochem.*, 29(5-7-7 pt 2), 1163–1179, doi:10.1016/S0146-6380(98)00062-X,
1377 1998.
- 1378 Wada, H., and Murata, N.: Lipids in thylakoid membranes and photosynthetic cells, In: *Lipids in Photosynthesis*, Springer,
1379 Dordrecht, 1-9, https://doi.org/10.1007/978-90-481-2862-1_1, 2009.
- 1380 Wagner, S., Schubotz, F., Kaiser, K., Hallmann, C., Waska, H., Rossel, P. E., Hansman, R., Elvert, M., Middelburg, J. J.,
1381 Engel, A., Blattmann, T. M., Catalá, T. S., Lennartz, S. T., Gomez-Saez, G. V., Pantoja-Gutiérrez, S., Bao, R. and Galy,
1382 V.: Soothsaying DOM: A Current Perspective on the Future of Oceanic Dissolved Organic Carbon, *Front. Mar. Sci.*,
1383 7(May), 1–17, doi:10.3389/fmars.2020.00341, 2020.
- 1384 Wakeham, S. G., Turich, C., Schubotz, F., Podlaska, A., Li, X. N., Varela, R., Astor, Y., Sáenz, J. P., Rush, D., Sinninghe
1385 Damsté, J. S., Summons, R. E., Scranton, M. I., Taylor, G. T. and Hinrichs, K. U.: Biomarkers, chemistry and
1386 microbiology show chemoautotrophy in a multilayer chemocline in the Cariaco Basin, *Deep. Res. Part I Oceanogr. Res.*
1387 *Pap.*, 63, 133–156, doi:10.1016/j.dsr.2012.01.005, 2012.
- 1388 Wang, X., Shen, Z. and Miao, X.: Nitrogen and hydrophosphate affects glycolipids composition in microalgae, *Sci. Rep.*,
1389 6(July), 1–9, doi:10.1038/srep30145, 2016.
- 1390 Wilhelm, C., Jungandreas, A., Jakob, T. and Goss, R.: Light acclimation in diatoms: From phenomenology to mechanisms,
1391 *Mar. Genomics*, 16(1), 5–15, doi:10.1016/j.margen.2013.12.003, 2014.
- 1392 Wörmer, L., Lipp, J. S., Schröder, J. M., Hinrichs, K. U.: Application of two new LC–ESI–MS methods for improved detection
1393 of intact polar lipids (IPLs) in environmental samples, *Org. Geochem.*, 59, 10-21,
1394 <https://doi.org/10.1016/j.orggeochem.2013.03.004>, 2013.
- 1395 Wörmer, L., Lipp, J. S., and Hinrichs, K. U.: Comprehensive analysis of microbial lipids in environmental samples through
1396 HPLC-MS protocols, in: *Hydrocarbon and lipid microbiology protocols*, Springer, Berlin, Heidelberg, 289-317,
1397 https://doi.org/10.1007/8623_2015_183, 2015.
- 1398 Wright, J. J., Konwar, K. M. and Hallam, S. J.: Microbial ecology of expanding oxygen minimum zones, *Nat. Rev. Microbiol.*,
1399 10(6), 381–394, doi:10.1038/nrmicro2778, 2012.
- 1400 Wu, R. S. S., Wo, K. T. and Chiu, J. M. Y.: Effects of hypoxia on growth of the diatom *Skeletonema costatum*, *J. Exp. Mar.*
1401 *Bio. Ecol.*, 420–421, 65–68, doi:10.1016/j.jembe.2012.04.003, 2012.
- 1402 Wyrтки, K.: The oxygen minima in relation to ocean circulation, *Deep. Res. Oceanogr. Abstr.*, 9(1–2), 11–23,
1403 doi:10.1016/0011-7471(62)90243-7, 1962.
- 1404 Yang, C., Boggasch, S., Haase, W. and Paulsen, H.: Thermal stability of trimeric light-harvesting chlorophyll a/b complex
1405 (LHCIIb) in liposomes of thylakoid lipids, *Biochim. Biophys. Acta - Bioenerg.*, 1757(12), 1642–1648,
1406 doi:10.1016/j.bbabi.2006.08.010, 2006.

- 1407 Yang, K. and Han, X.: Accurate quantification of lipid species by electrospray ionization mass spectrometry - Meets a key
1408 challenge in lipidomics, *Metabolites*, 1(1), 21–40, doi:10.3390/metabo1010021, 2011.
- 1409 Yang, W., Catalanotti, C., Wittkopp, T. M., Posewitz, M. C. and Grossman, A. R.: Algae after dark: Mechanisms to cope with
1410 anoxic/hypoxic conditions, *Plant J.*, 82(3), 481–503, doi:10.1111/tpj.12823, 2015.
- 1411 Yeesang, C. and Cheirsilp, B.: Effect of nitrogen, salt, and iron content in the growth medium and light intensity on lipid
1412 production by microalgae isolated from freshwater sources in Thailand, *Bioresour. Technol.*, 102(3), 3034–3040,
1413 doi:10.1016/j.biortech.2010.10.013, 2011.
- 1414 Yoon, K., Han, D., Li, Y., Sommerfeld, M. and Hu, Q.: Phospholipid:Diacylglycerol acyltransferase is a multifunctional
1415 enzyme involved in membrane lipid turnover and degradation while synthesizing triacylglycerol in the unicellular green
1416 microalga *chlamydomonas reinhardtii*, *Plant Cell*, 24(9), 3708–3724, doi:10.1105/tpc.112.100701, 2012.
- 1417 Yvon-Durocher, G., Allen, A. P., Cellamare, M., Dossena, M., Gaston, K. J., Leitao, M., Montoya, J. M., Reuman, D. C.,
1418 Woodward, G. and Trimmer, M.: Five Years of Experimental Warming Increases the Biodiversity and Productivity of
1419 Phytoplankton, *PLoS Biol.*, 13(12), 1–22, doi:10.1371/journal.pbio.1002324, 2015.
- 1420 Zienkiewicz, K., Du, Z. Y., Ma, W., Vollheyde, K. and Benning, C.: Stress-induced neutral lipid biosynthesis in microalgae
1421 — Molecular, cellular and physiological insights, *Biochim. Biophys. Acta - Mol. Cell Biol. Lipids*, 1861(9), 1269–1281,
1422 doi:10.1016/j.bbalip.2016.02.008, 2016.
- 1423 Zink K-G, Wilkes H, Disko U, Elvert M, Horsfield B. Intact phospholipids—microbial “life markers” in marine deep
1424 subsurface sediments. *Org. Geochem*; 34: 755-769, [https://doi.org/10.1016/S0146-6380\(03\)00041-X](https://doi.org/10.1016/S0146-6380(03)00041-X), 2003.

1425 **Tables**

1426

1427 **Table 1: Concentration of inorganic nutrients ($\mu\text{mol/L}$), nutrient stoichiometry, and pH_T of the two batches of ODZ**
1428 **water collected and added to the mesocosm experiment.**

	Si(OH)_4	PO_4^{3-}	NO_2^-	NH_4^+	NO_3^-	N:P:Si	pH_T	Depth (m)
Station 1	17.4	2.6	0	0.3	0	0.1:1.0:6.7	7.47	30
Station 3	19.6	2.5	2.9	0.3	1.1	1.7:1.0:7.8	7.49	70

1430

1431

1432

1433

1434

1435

1436

1437 **Table 2: IPL classes included in this study and their respective acronyms.**

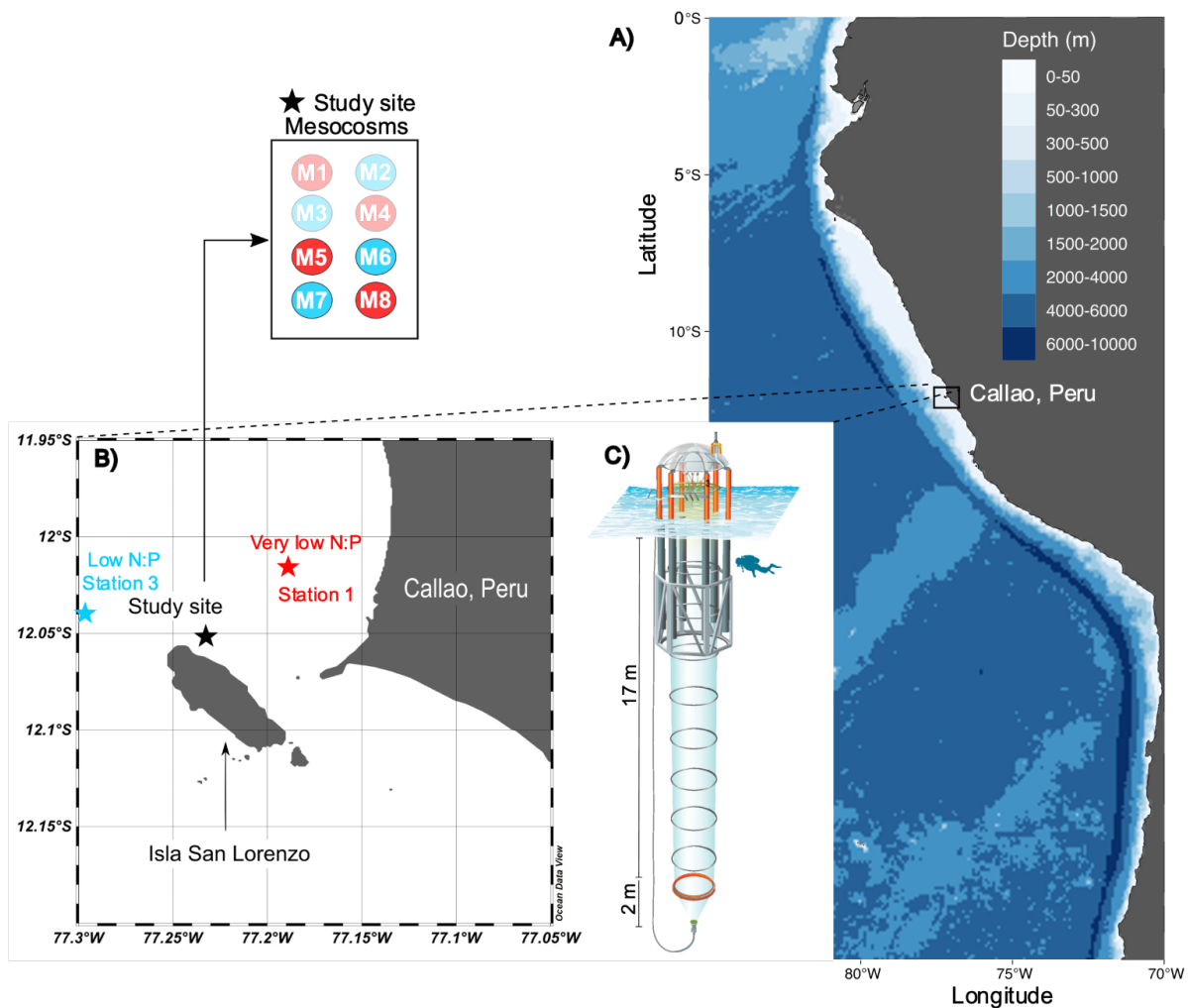
IPL Headgroups	Acronym	IPL Category
Digalactosyldiacylglycerol	DGDG	Glycolipid
Monogalactosyldiacylglycerol	MGDG	Glycolipid
Sulfoquinovosyldiacylglycerol	SQDG	Glycolipid
Phosphatidylglycerol	PG	Phospholipid
Phosphatidylcholine	PC	Phospholipid
Phosphatidylethanolamine	PE	Phospholipid
Diacylglyceryl trimethylhomoserine	DGTS	Betaine Lipid
Diacylglyceryl hydroxymethyl-trimethyl-beta-alanine	DGTA	Betaine Lipid
Diacylglyceryl carboxyhydroxymethylcholine	DGCC	Betaine Lipid

1438

1439

1440 **Figures**

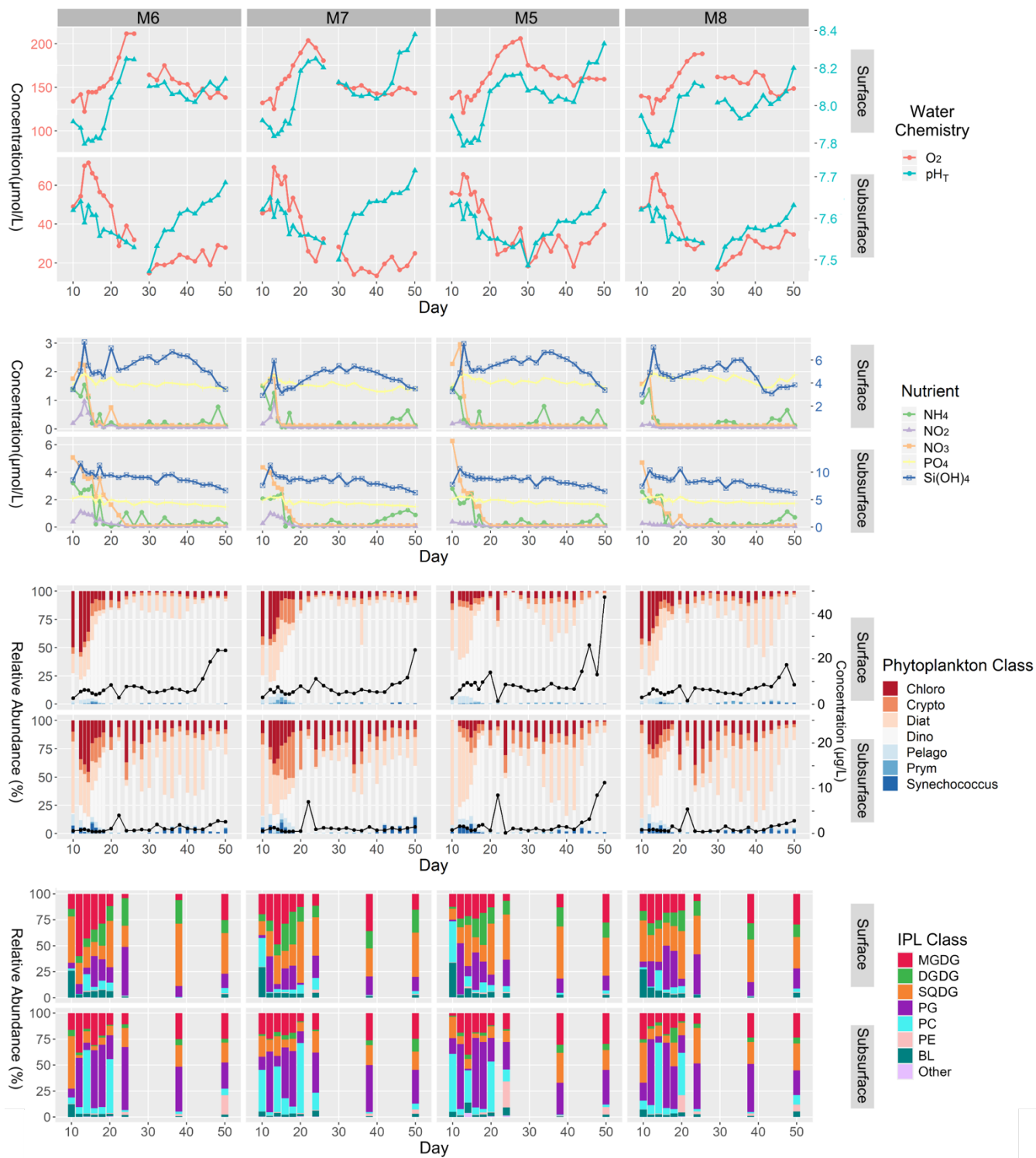
1441



1442
 1443
 1444
 1445
 1446
 1447

Figure 1: The KOSMOS study site. (A) Overview map indicating the location of the study region in La Punta, Callao, Perú. (B) Detailed map of the study site with the mesocosm arrangement (M1-8). Red (very low N:P) and blue (low N:P) colors indicate the different stations for ODZ water collection (1 and 3; star symbols) and replicates of the two different water treatments (numbers in circles in insert). (C) Diagram of a mesocosm unit with underwater bag dimensions. Modified figure from Chen et al. (2022).

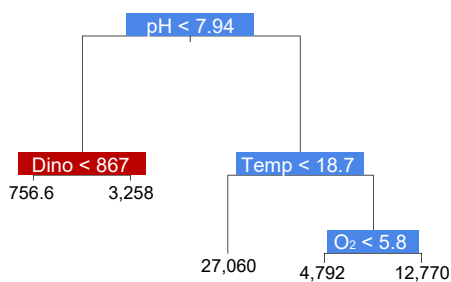
1448
 1449



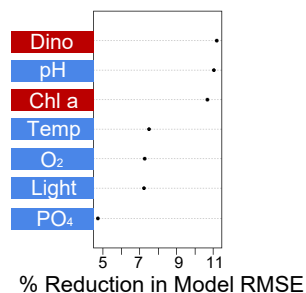
1450

1451

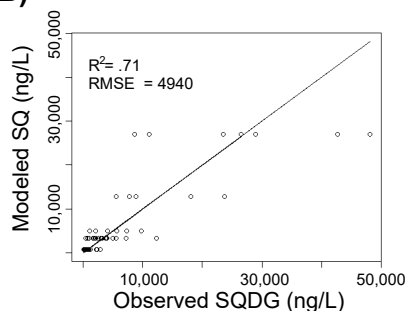
A) Pruned Tree SQDG



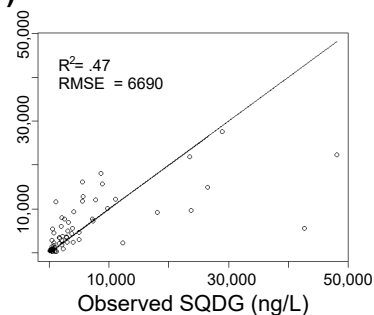
C) Random Forest SQDG



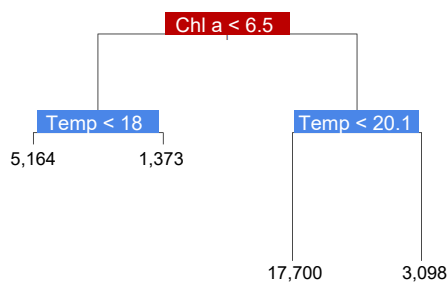
B)



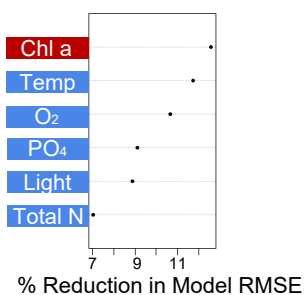
D)



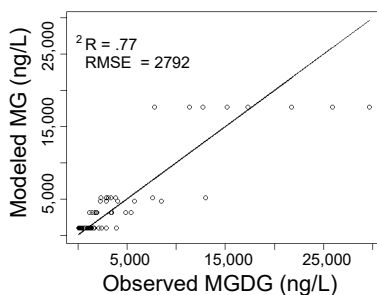
E) Pruned Tree MGDG



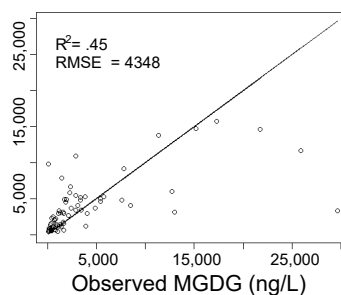
G) Random Forest MGDG



F)



H)

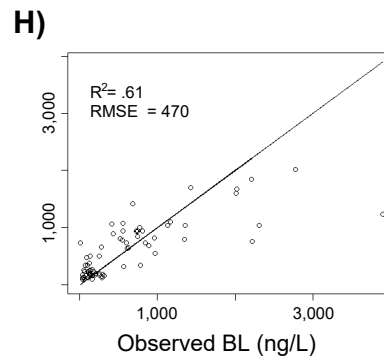
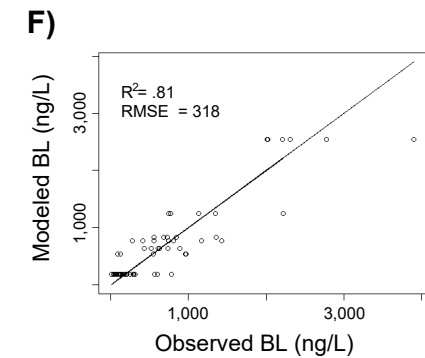
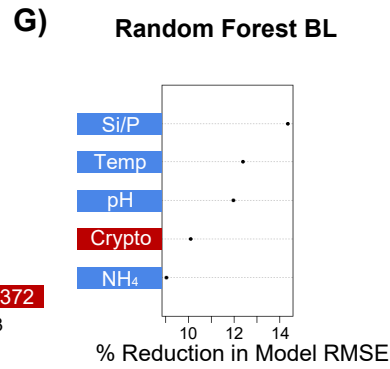
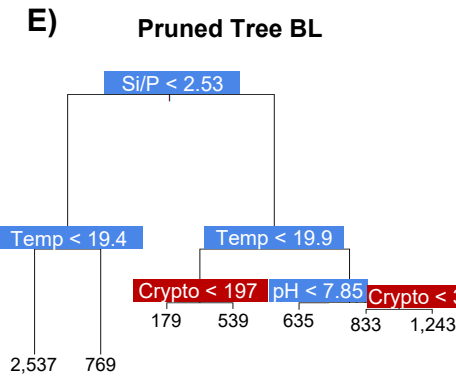
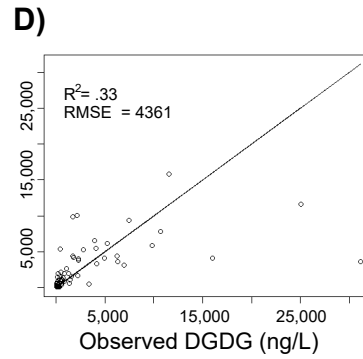
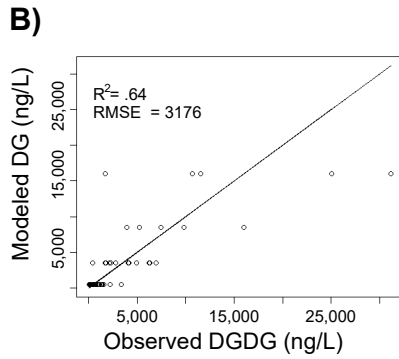
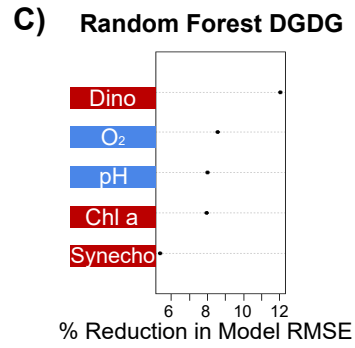
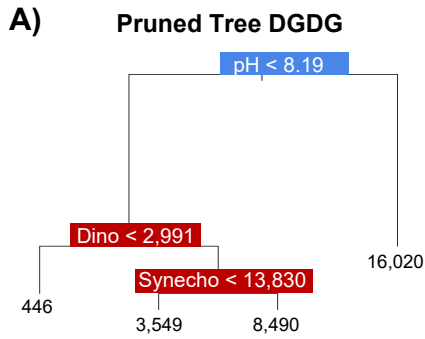


1466 **Figure 4: Classification and Regression Tree (CART) and Random Forest analyses of selected IPL classes (Top: SQDG; Bottom:**
1467 **MGDG). A and E indicate a summary of primary predictors in the best fit CART (i.e. Pruned Tree), whereas B and F show model**
1468 **performance via adjusted R² and RMSE. C and G display Random Forest variable importance in the prediction of IPL classes as**
1469 **defined by % reduction in RMSE, whereas D and H show model performance via adjusted R² and RMSE. Environmental variables**
1470 **are depicted in blue, whereas biological variables are shown in red for both analyses.**

1471

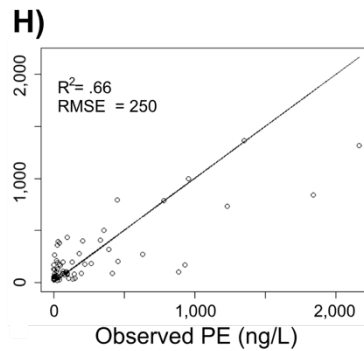
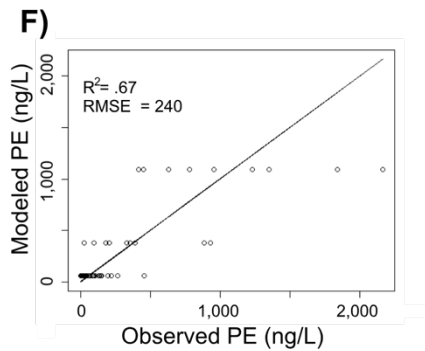
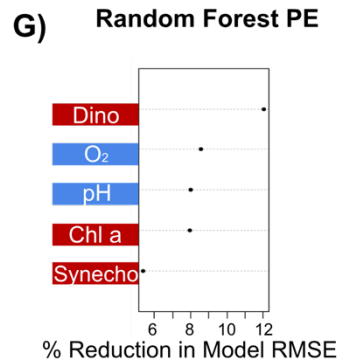
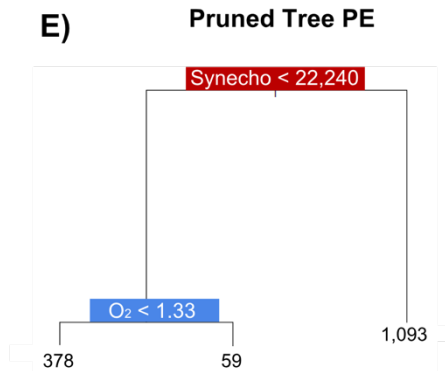
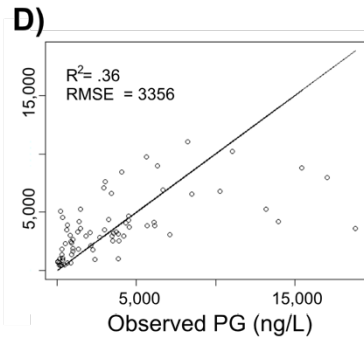
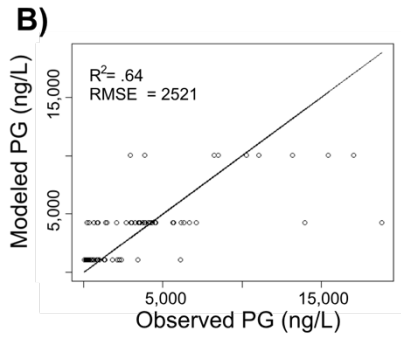
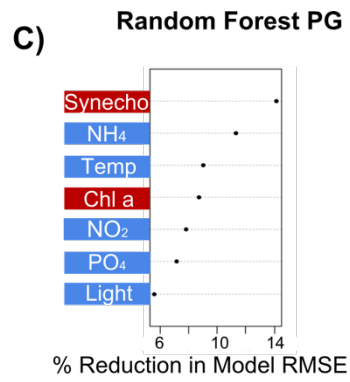
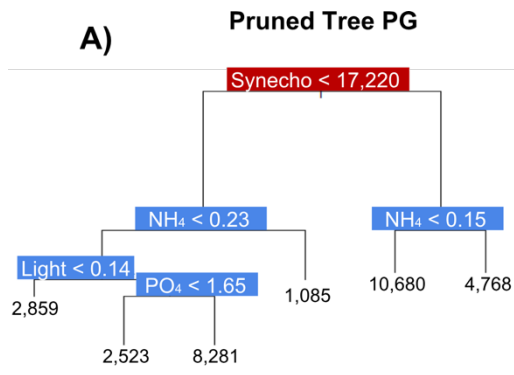
1472

1473



1475 **Figure 5: Classification and Regression Tree (CART) and Random Forest analyses of selected IPL classes (Top: DGDG; Bottom:**
1476 **BL). A and E indicate a summary of primary predictors in the best fit CART (i.e. Pruned Tree), whereas B and F show model**
1477 **performance via adjusted R² and RMSE. C and G display Random Forest variable importance in the prediction of IPL classes as**
1478 **defined by % reduction in RMSE, whereas D and H show model performance via adjusted R² and RMSE. Environmental variables**
1479 **are depicted in blue, whereas biological variables are shown in red for both analyses.**

1480

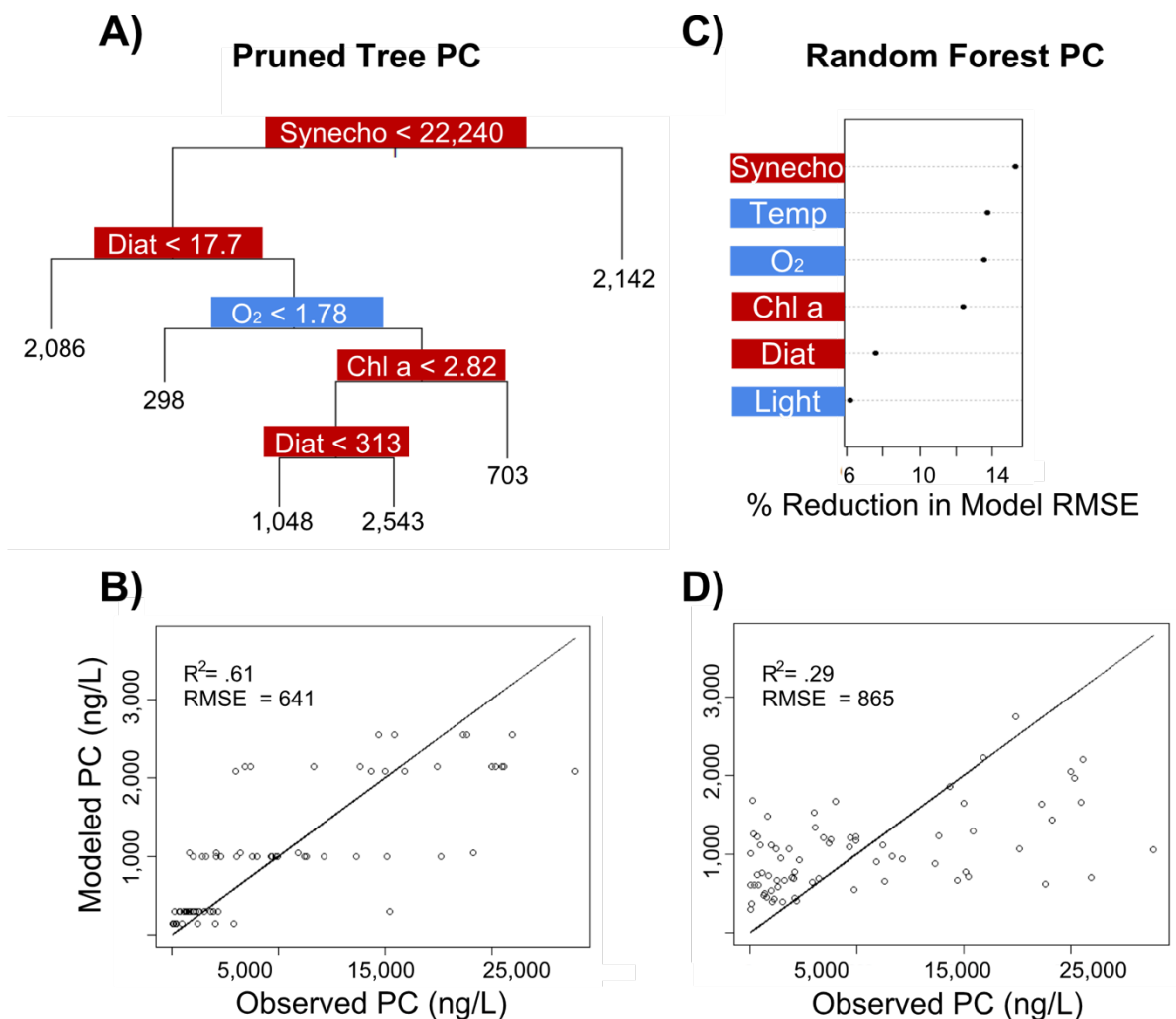


1482 Figure 6: Classification and Regression Tree (CART) and Random Forest analyses of selected IPL classes (Top: PG; Bottom: PE).
 1483 A and E indicate a summary of primary predictors in the best fit CART (i.e. Pruned Tree), whereas B and F show model performance
 1484 via adjusted R^2 and RMSE. C and G display Random Forest variable importance in the prediction of IPL classes as defined by %
 1485 reduction in RMSE, whereas D and H show model performance via adjusted R^2 and RMSE. Environmental variables are depicted
 1486 in blue, whereas biological variables are shown in red for both analyses.

1487

1488

1489



1490

1491 Figure 7: Classification and Regression Tree (CART) and Random Forest analyses of selected IPL classes (PC). A indicate a
 1492 summary of primary predictors in the best fit CART (i.e. Pruned Tree), whereas B shows model performance via adjusted R^2 and
 1493 RMSE. C and G display Random Forest variable importance in the prediction of IPL classes as defined by % reduction in RMSE,
 1494 whereas D show model performance via adjusted R^2 and RMSE. Environmental variables are depicted in blue, whereas biological
 1495 variables are shown in red for both analyses.

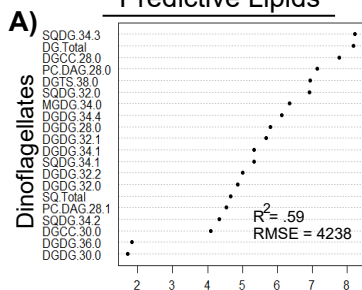
1496

1497
1498

Predictive Lipids

Dominant IPL Classes

Potential IPL Remodeling



SQDG, DGDG

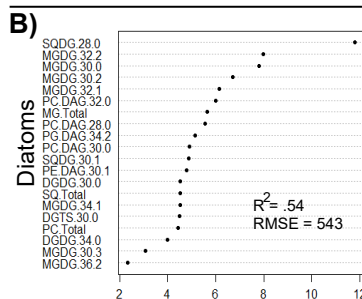
Recycling of PC and BL under N-limitation

Recycling of MGDG under high pH/low pCO₂, or anaerobiosis

Increased proportion of DGDG and SQDG under thermal stress or high pH/low pCO₂

Increased proportion of SQDG under shaded conditions

Recycling of MGDG and PG under high growth conditions



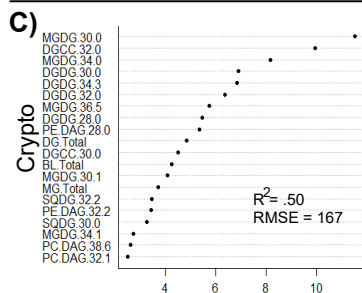
MGDG, SQDG, PC

Recycling of BL under N-limitation

Increased proportion of SQDG under thermal stress, shaded conditions, and high pH/low pCO₂

Increased proportion of MGDG for photoprotective and antioxidant mechanisms

Recycling of PG under high growth conditions



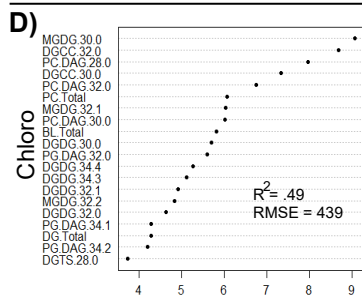
BL, DGDG, MGDG

Recycling of PC under N-limitation

Enhanced DGDG under thermal stress

Enhanced MGDG for photoprotective and antioxidant mechanisms

Recycling of SQDG and PG under high growth conditions

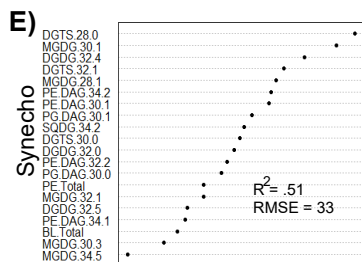


PC, BL, DGDG

Recycling of MGDG under high pH/low pCO₂ or anaerobiosis

Enhanced DGDG under thermal stress

Recycling of SQDG, MGDG, and PG under high growth conditions



PE, BL

Recycling of PC under N-limitation

Recycling of MGDG under high pH/low pCO₂ or anaerobiosis

Increased proportion of SQDG under shaded conditions

Recycling of SQDG, MGDG, and PG under high growth conditions

% Reduction in Model RMSE

1500 **Figure 8: Random Forest-based identification of the 15 most important individual IPLs in the prediction of phytoplankton groups.**
1501 **Dominant IPL classes and the potential remodeling advantages for each group are summarized. The nomenclature of IPL molecules**
1502 **follows that of the main text, starting with the type of headgroup, followed by the number of carbon atoms in fatty acid chains, and**
1503 **the total number of double bonds in the fatty acid chains. The root mean square error (RMSE) of random forest models is defined**
1504 **as ng/L of chl-a, and coefficient of determination (R^2) provided for each model fit.**